RESILIENCE OF MICROGRID DURING CATASTROPHIC EVENTS

Travis Black

Thesis Prepared for the Degree of

MASTER OF SCIENCE

UNIVERSITY OF NORTH TEXAS

May 2018

APPROVED:

Miguel Acevedo, Major Professor
Xiangnan Zhong, Committee Member
Tao Yang, Committee Member
Shengli Fu, Chair of the Department of Electrical Engineering
Costas Tsatsoulis, Dean of the College of Engineering
Victor Prybutok, Dean of the Toulouse Graduate School

Black, Travis. *Resilience of Microgrid during Catastrophic Events*. Master of Science (Electrical Engineering), May 2018, 70 pp., 2 tables, 48 figures, 21 numbered references.

Today, there is a growing number of buildings in a neighborhood and business parks that are utilizing renewable energy generation, to reduce their electric bill and carbon footprint. The most current way of implementing a renewable energy generation is to use solar panels or a windmill to generate power; then use a charge controller connected to a battery bank to store power. Once stored, the user can then access a clean source of power from these batteries instead of the main power grid. This type of power structure is utilizing a single module system in respect of one building. As the industry of renewable power generation continues to increase, we start to see a new way of implementing the infrastructure of the power system. Instead of having just individual buildings generating power, storing power, using power, and selling power there is a fifth step that can be added, sharing power. The idea of multiple buildings connected to each other to share power has been named a microgrid by the power community. With this ability to share power in a microgrid system, a catastrophic event which cause shutdowns of power production can be better managed. This paper then discusses the data from simulations and a built physical model of a resilient microgrid utilizing these principles.

Copyright 2018

by

Travis Black

ACKNOWLEDGMENTS

I would like to take the time to express my gratitude to a multitude of individuals that assisted in making my master's thesis a reality. First, I would like to thank my faculty advisor, Dr. Miguel Acevedo, who was a pillar to the project by mentoring and guiding me through the thesis process of different theoretical concepts about solar panels, windmills, and batteries to the concepts of different gauge wire. I am quite certain the microgrid would not have been created if not for Dr. Acevedo's vast knowledge and assistance. If Dr. Acevedo was the pillar to this microgrid, then Ms. Breana Smithers was the concrete base. Ms. Smithers helped me in scheduling, ordering, and assembling the physical model of the microgrid. During the process of building and simulating the microgrid, my two thesis advisors, Dr. Tao Yang and Dr. Xiangnan Zhong, where invaluable to the process as a source of great knowledge and appropriate suggestions. I give very special thanks to Dr. Yang for financing the building of the microgrid with the collaboration of Dr. Acevedo and the University of North Texas (UNT) Electrical Engineering Department. I would also like to give a special thanks to UNT Electrical Engineering Department's office staff Jason Mieritz, Peggy Foster, and Stacey Janczak. Their continued guidance in advising, friendly conversations, and speedy assistance in every academic need I had freed me to focus on my classes and thesis. Lastly, I would like to give a special thanks to Kelvin Darden and Jyothis Joseph who have been good friends and students as I worked my way through my graduate degree. Kelvin and Jyothis both helped assemble the microgrid, as well as, learned with me how to use the microgrid model for a specialized thesis topic.

TABLE OF CONTENTS

Page

ACKNOWLEDGMENTS iii

LIST OF TABLES vi

LIST OF FIGURES vii

CHAPTER 1. INTRODUCTION 1

1.1 Background 1

1.2 Motivation 2

1.3 Objective 2

1.4 Chapters Overview 3

CHAPTER 2. RENEWABLE POWER GENERATORING FOR SINGLE SYSTEM 4

2.1 Introduction 4

2.2 Photovoltaic Panels 4

2.3 Wind Turbines or Wind Mills 8

2.4 Rechargeable Battery Banks 9

2.5 Charge Controllers 11

2.6 Inverters 12

CHAPTER 3. MICROGRID PHYSICAL MODEL 14

3.1 Introduction 14

3.2 Physical Components of Microgrid Model 15

3.2.1 Talesun TP672P-320 Photovoltaic Panel 15

3.2.2 Crown CR-GC150 Deep Cycle Batteries 16

3.2.3 Morningstar TriStar MPPT Solar Charge Controller 16

3.2.4 Solar Panel Mounts 17

3.2.5 12x16x7 Metal Shed 19

3.2.6 1000-Watt Twin-Head Halogen Yellow Work Lights 19

3.2.7 Samlex PSE-24125A 1250W & Samlex PST-600-24 600W Inverters 20

3.2.8 Miscellaneous 21

3.3 Microgrid Site Layout 23

3.4 Mounting System for Microgrid's Solar Panel Array 23

3.5 Block and Wiring Diagrams of Microgrid Model 24
3.6 Microgrid Model Expenses 24

CHAPTER 4. SIMULATED SINGLE SYSTEM AND MICROGRID 29
4.1 Introduction 29
4.2 Simulink Model Parts 29
4.2.1 Entire Microgrid Model Overview 29
4.2.2 Solar Panel 31
4.2.3 Battery and Battery Controller 33
4.2.4 Loads 36
4.2.5 Grid 37
4.2.6 Scenario 39
4.3 Simulink Model Results 41
4.4 SAM's Breakdown for a House 47
4.5 SAM Output for a House 49

CHAPTER 5. PHYSICAL MICROGRID MODEL DATA 54
5.1 Isolated Nodes (No Microgrid) 54
5.1.1 Rainy Day – No Loads – Large Node 54
5.1.2 Rainy Day – No Loads – Small Node 56
5.1.3 Sunny Day – No Loads – Large Node 57
5.1.4 Sunny Day – No Loads – Small Node 58
5.1.5 Sunny Day – With Loads – Large Node 59
5.1.6 Sunny Day – With Loads – Small Node 60
5.2 Combined Nodes (Microgrid) 61
5.2.1 Sunny Day – With Loads – Large Node 61
5.2.2 Partly Cloudy Day – With Loads – Small Node 63
5.2.3 Sunny Day – With Loads – Small Node – Small Array Shutdown 64

CHAPTER 6. CONCLUSION AND FUTURE IMPLEMENTATION 66
6.1 Conclusion 66
6.2 Future Implementations 67

REFERENCES 69

LIST OF TABLES

Page

Table 3.1 : Microgrid model expenses..... 27

Table 4.1 : SAM simulation overview table 50

LIST OF FIGURES

Page

Figure 2.1 : LTSpice solar cell circuit 5

Figure 2.2 : LTSpice solar panel circuit..... 6

Figure 2.3 : LTSpice solar panel I vs. V curve 7

Figure 2.4 : LTSpice solar panel P vs. V curve 7

Figure 2.5 : Graph of power vs. wind speed for wind turbines 9

Figure 2.6 : SOC of lead acid batteries graph..... 10

Figure 2.7 : Lead acid battery voltage vs. discharge capacity % graph..... 10

Figure 2.8 : Lithium ion voltage vs. discharge capacity graph..... 11

Figure 2.9 : Inverter positive to negative power flow..... 13

Figure 2.10 : Inverter negative to positive power flow..... 13

Figure 3.1 : Talesun TP672P-320 solar panel..... 15

Figure 3.2 : Crown CR-GC150 deep cycle battery..... 16

Figure 3.3 : Morningstar TriStar MPPT solar charge controller 17

Figure 3.4 : Solar panel mounts..... 18

Figure 3.5 : 1000W twin-head halogen yellow work light..... 20

Figure 3.6 : Samlex power 600W & 1250W inverters 21

Figure 3.7 : UNT Discovery Park's microgrid site layout..... 22

Figure 3.8 : Solar panel mounts front view (drawn by Breana Smithers) 23

Figure 3.9 : Solar panel mounts side view (drawn by Breana Smithers)..... 24

Figure 3.10 : Block diagram of physical microgrid model..... 25

Figure 3.11 : LTSpice wiring diagram for entire microgrid model 26

Figure 4.1 : Simulink microgrid model..... 30

Figure 4.2 : Simulink solar panel block..... 32

Figure 4.3 : Simulink circuitry of solar panel block 33

Figure 4.4 : Simulink battery block 34

Figure 4.5 : Simulink battery controller block 35

Figure 4.6 : Simulink circuitry of Battery Control block 35

Figure 4.7 : Simulink load block 37

Figure 4.8 : Simulink circuitry of load block 37

Figure 4.9 : Simulink main grid block 38

Figure 4.10 : Simulink scenario block 39

Figure 4.11 : Simulink conditions of the scenario block 40

Figure 4.12 : Simulink module 1 output graphs (normal operation) 42

Figure 4.13 : Simulink module 2 output graphs (normal operation) 43

Figure 4.14 : Simulink module 3 output graphs (normal operation) 44

Figure 4.15 : Simulink module 1 output graph (6 hours of PV shut off time) 46

Figure 4.16 : SAM monthly energy production graph 51

Figure 4.17 : SAM monthly energy and load graph 52

Figure 4.18 : SAM monthly solar array and load energy vs. time graphs 53

Figure 5.1 : Excel graph of node 3 (large node) rainy day with no loads 55

Figure 5.2 : Excel graph of node 2 (small node) rainy day with no loads 56

Figure 5.3 : Excel graph of node 3 (large node) sunny day with no loads 57

Figure 5.4 : Excel graph of node 2 (small node) sunny day with no loads 58

Figure 5.5 : Excel graph of node 3 (large node) sunny day with loads 59

Figure 5.6 : Excel graph of node 2 (small node) sunny day with loads 60

Figure 5.7 : Excel graph of node 3 (large node) sunny day with loads using microgrid 62

Figure 5.8 : Excel graph of node 2 (small node) partly cloudy day with loads using microgrid .. 63

Figure 5.9 : Excel graph of node 2 (small node) sunny day with loads using microgrid and one small solar array shutdown 64

CHAPTER 1

INTRODUCTION

1.1 Background

Today, there is a growing number of houses in a neighborhood and business parks utilizing renewable energy generation, to reduce their electric bill and carbon footprint. The most current way of implementing renewable energy generation is to use solar panels or a windmill to generate power; then use a charge controller connected to a battery bank to store power. Once stored, the user can then access a clean source of power from these batteries instead of the main power grid. If the renewable energy generators generate more power than what the battery banks can hold, then the user can sell the extra power to the main grid. Which means the user will add electricity to the main grid instead of take electricity from it [1].

As the industry of renewable power generation continues to increase, we start to see a new way of implementing the infrastructure of the power system. Instead of having just individual building generating power, storing power, using power, and selling power there is a fifth step that can be added, sharing power. Instead of immediately selling your excess power to the main grid, share it with your neighboring buildings. A multitude of buildings generate power from renewable generators, store power in a battery bank, use power in the buildings' loads, share excess power to neighboring buildings that need it, and sell whatever power is left to the main grid. The idea has been named a microgrid by the power community and is what this thesis paper is about [2].

1.2 Motivation

Another key benefit of these renewable energy generators is, even during blackouts (when the main grid is shut-down), these buildings still have a way to access power either from the stored power in the battery banks or the renewable energy generators that they have on site [3]. However, even if one building has the benefits of having power during blackouts, which can be caused by a multitude of events, what about other neighboring houses? The idea of the microgrid really shines because now instead of power being supplied by one house, you can have power coming from a multitude of nearby buildings with their own renewable energy generators. What makes microgrids so interesting and resilient against the main grid possible shut downs [4]? The idea of resiliency of the microgrid was what motivated this project, which led to the study and data collection. Take for instance, there is an earthquake in California and the main power grid is damaged leading to many houses and buildings power outage. Which can be catastrophic for the modern human because most of our daily lives revolve around electrical devices. Furthermore, without electricity in that area the cleanup process would take even longer, not to mention the money lost for local businesses that require electrical devices to stay in operation [5] like food storage, financial institutions, online retailers, and gas stations.

1.3 Objective

The goals of this thesis include:

- To simulate a microgrid with three modules (houses) that generate, store, use, and share power using renewable generators.
- To build a physical model of three nodes that generate, store, use, and share power using solar panels or wind mills.

- To gain data from the physical model and see if it was truly resilient against unforeseen power shutdowns or shortages.
- To simulate in the physical model of a microgrid that was already disconnected to the main grid and make sure it was still resilient.
- To gain useful data about how microgrids operate in real life compared to simulations.

1.4 Chapters Overview

Chapter 2 provides useful information and reviews how different renewable generators and components operate in a single renewable generating house.

Chapter 3 goes into depth about how the different components in the microgrid operate and how they are used.

Chapter 4 describes the different simulations generated by explaining how they work corresponding to the outputs.

Chapter 5 presents what data was gathered from the physical microgrid model and how it compared to the simulations of the microgrid.

Chapter 6 talks about the conclusion, future expansion, and suggestions to improve the design of a resilient microgrid.

CHAPTER 2

RENEWABLE POWER GENERATORING FOR SINGLE SYSTEM

2.1 Introduction

Currently in the market of renewable power, there are two options for the average consumer to buy. These are photovoltaic (PV) panels and wind turbines (wind mills). These generators generate the necessary power either from solar radiation in the case of PV panels, or using wind in the case of wind turbines. Both generators have their strengths and weaknesses on how they generate their power, which sections 2.2 and 2.3 will describe in more depth. Generated power needs to be used instantly or it can be stored in a battery bank for later use. Section 2.4 will go into more depth about batteries and the different kind of batteries you can use. These battery banks can be charged and not overcharged thanks to a device called a charge controller. There are a few different charge controllers, which will be discussed in section 2.5. Batteries are then used to provide the power to their connected loads. The power for the load can be in Direct Current (DC) straight from the battery banks or in Alternating Current (AC). For the power to be in AC inverters are added to the battery bank. Section 2.6 will explain how an inverter works and how it is used in a single renewable generating system.

2.2 Photovoltaic Panels

Photovoltaic (PV) panels work by creating electricity from the solar radiation received on the Earth’s surface. It works by the panel having a multitude of solar cells, which are each made up of semiconductor material based on silicon. When these cells receive photons of the required wavelength, the cells are energized, and electrons can move to the conduction band. The panels

then have a series of thin metal allowing free moving electrons a path to provide electric current and voltage to a load.

In Figure 2.1, using LTSpice a user can simulate a solar cell [6]. The solar cell was comprised of a diode (Dpv), two resistors (Rp & Rs), a current source (Epv), and a voltage dependent voltage source (Epv). Then in Figure 2.2, the same solar cell was made into an LTSpice module called PVModule. The module is then being connected to a current input source (Isc) with 5A. The PVModule's Vpv- will go to ground, and Pvp+ was connected to a load resistor, as well as, a 12-volt (V) output voltage source.

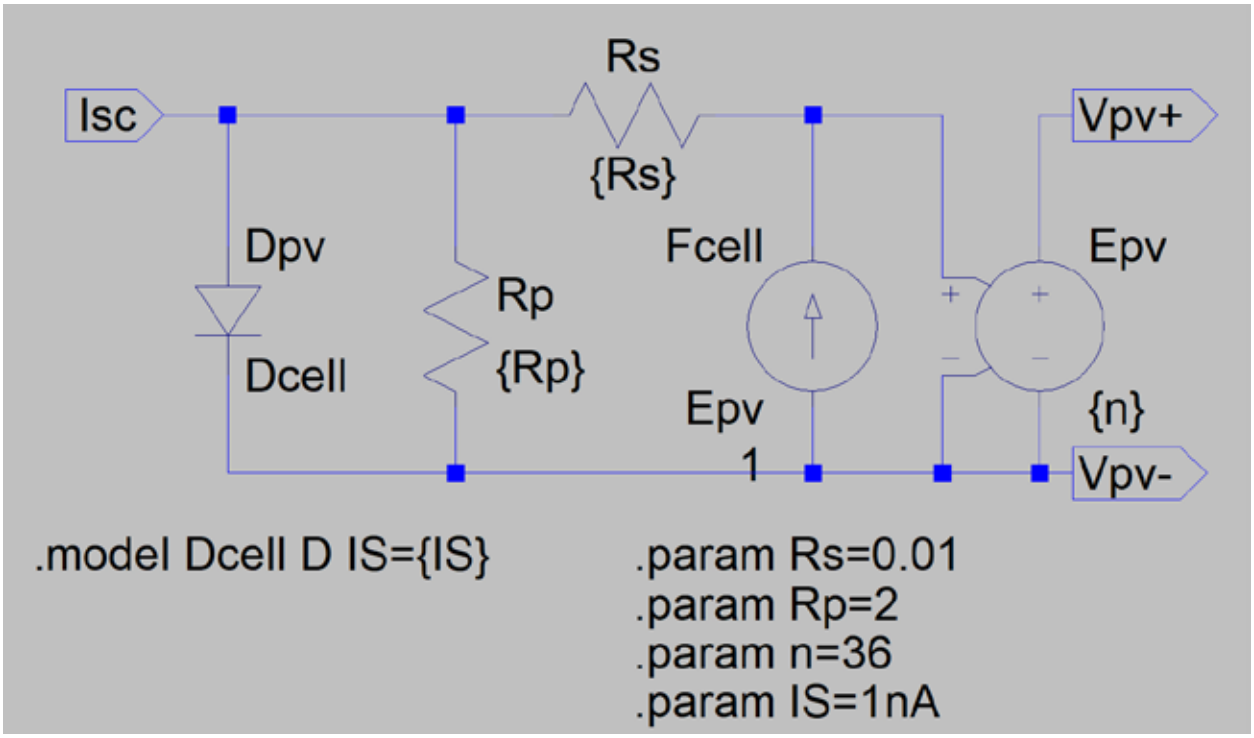

Figure 2.1 : LTSpice solar cell circuit

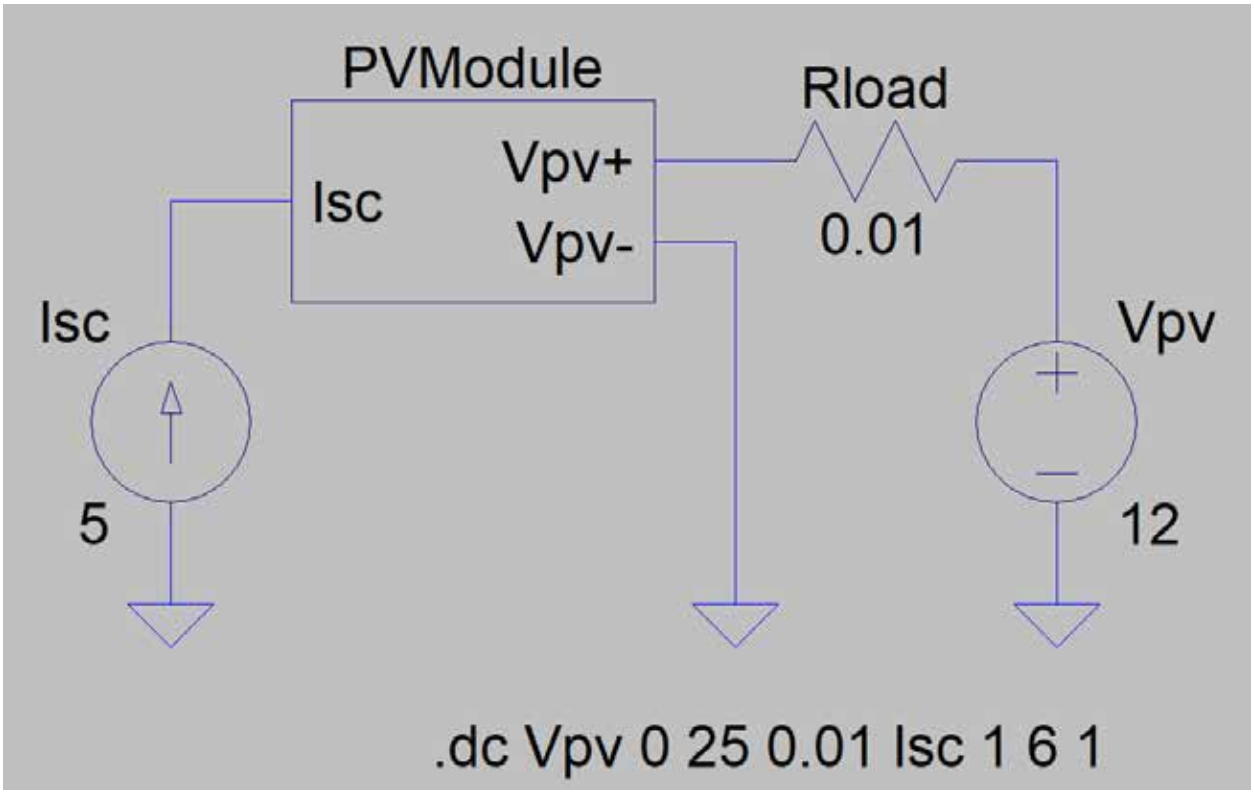

Figure 2.2 : LTSpice solar panel circuit

Using DC sweep the user can change the voltage of the input current source from 1 to 6 V with increments of 1, then change the voltage of the output voltage source from 0 to 25 V with increments of 0.01. It will generate a current vs. voltage (IV) curve of the solar panels, shown in Figure 2.3. Changing the axis values in LTSpice will also allow the power vs. voltage (P vs. V) curve to be seen in Figure 2.4. Using the PV curve, you can find the Maximum Power Point (MPP) of the graph given the different input voltages. The maximum point on the graph was where the voltage and current of the panel peaked and desired most in solar generation.

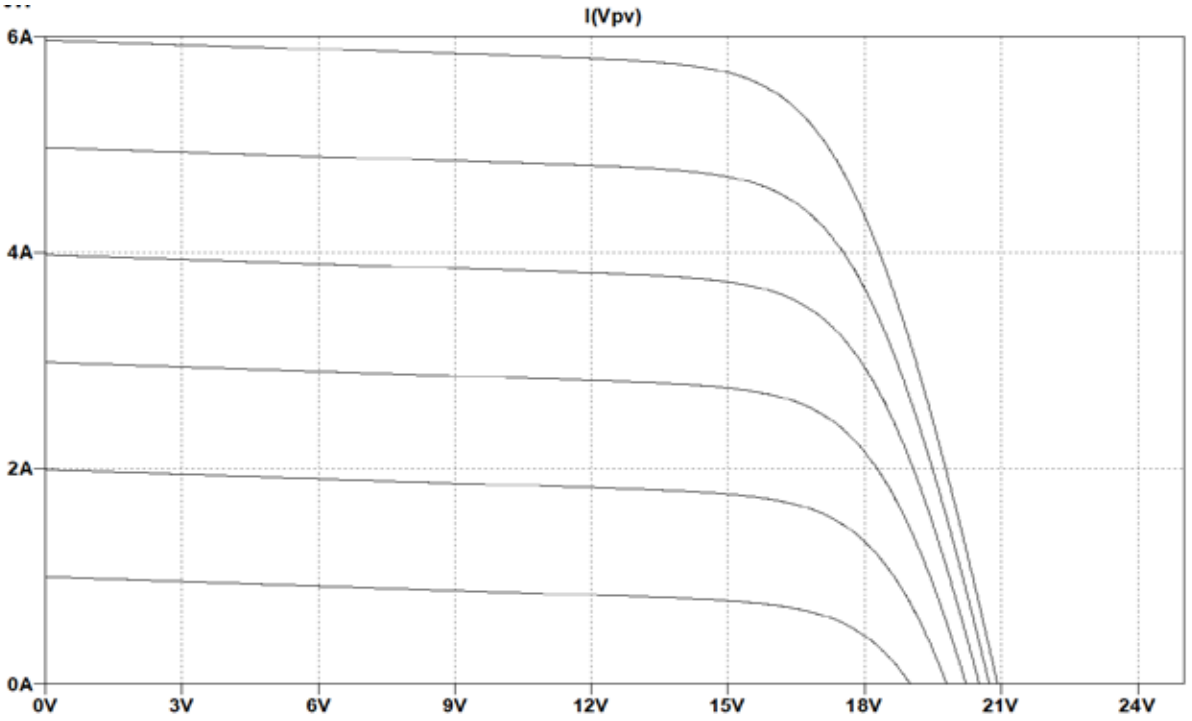

Figure 2.3 : LTSpice solar panel I vs. V curve

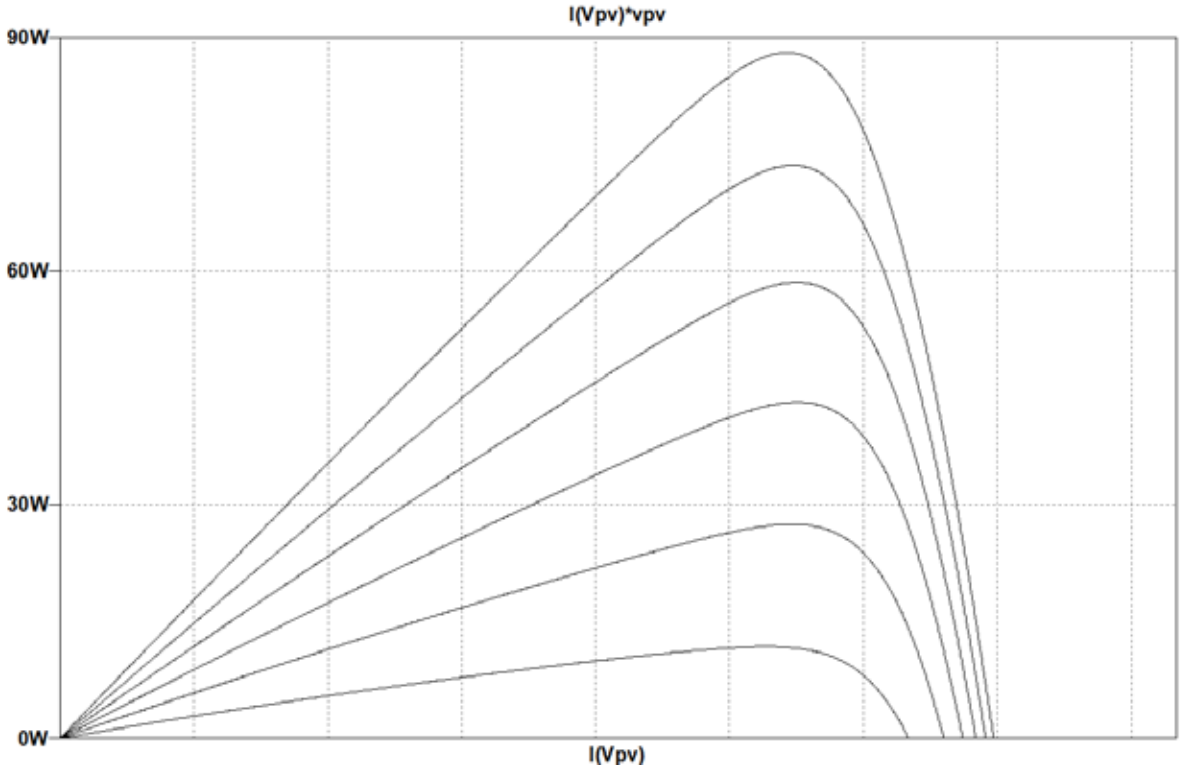

Figure 2.4 : LTSpice solar panel P vs. V curve

2.3 Wind Turbines or Wind Mills

The second most common renewable generator is the wind turbine or windmill. Wind turbines operate by having blades either horizontally or vertically. Using these blades, the wind turbine spins a generator that induces electrical current by the generator having rotating magnets that created an alternating current by spinning around an electrical wire. However, to store the power being generated by the wind turbine you need to convert the AC power to DC, usually done by a diode bridge rectifier.

There are three stages during the normal operation of a windmill. The first is below the cut-in wind speed stage where the speed of the wind is not great enough to spin the turbine's generator because the generator has resistance to spin thanks to friction and the magnetic field that wants to stay constant. Once the wind speed reaches a certain point, the wind turbine starts spinning. When the turbine starts spinning it will generate power non-linearly with respect to the wind speed, increasing until the turbine reaches the second stage of operation, which is the rated wind speed. The turbine does not increase its power but rather stays constant with respect to wind speed, which is the optimal stage of operation for wind turbines. However, if the wind speed becomes too great, the final stage that a wind turbine enters is above the cut-out wind speed when there is no power being generated and the turbine spins freely because when generating power beyond the limitations of the generator it may damage the generator. Figure 2.5 displays a graph of the different stages in the context of power vs wind speed [7].

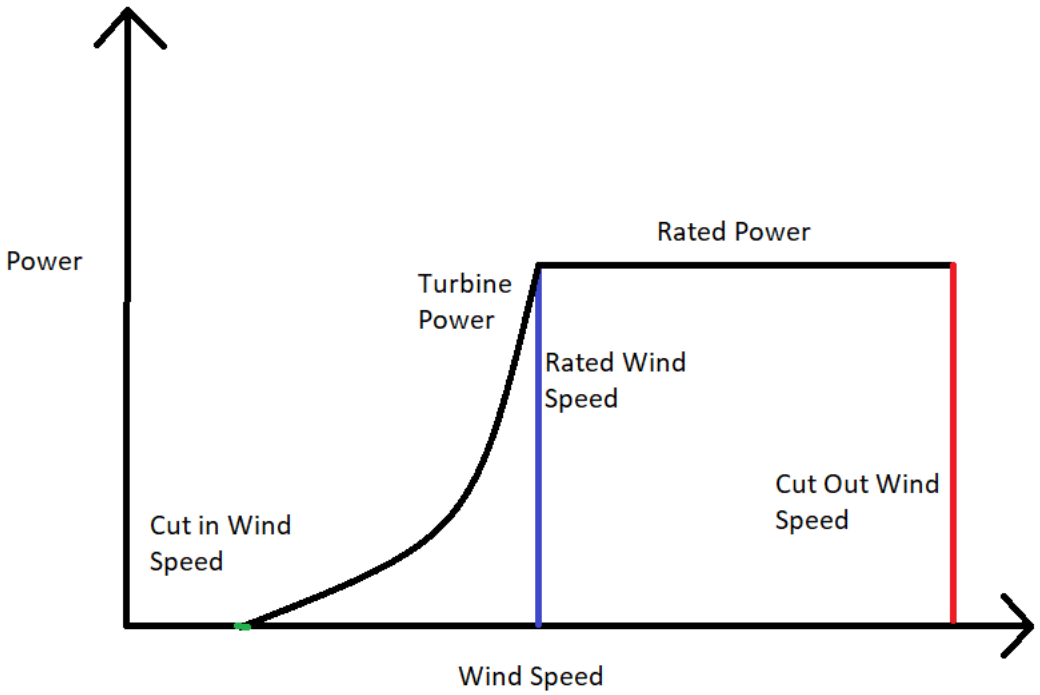

Figure 2.5 : Graph of power vs. wind speed for wind turbines

2.4 Rechargeable Battery Banks

Rechargeable batteries are the most common device used to store electricity. For renewable generating systems, batteries are connected in series or parallel to make battery banks. These banks are connected to charge controllers and store the power from the renewable generators. The battery banks allow a renewable generation system a power supply when the renewable generators are unable to generate power. Currently, in most renewable power generating systems, the batteries used for the battery banks are lead acid or lithium ion. Both battery types have different properties such as, state of charge (SOC) [8] and state of discharge (SOD). The relationship of SOC and SOD is direct because SOD equals 100 minus SOC. Lead acid batteries have a large change in the voltage as the state of charge increases (Figure 2.6).

State of discharge of a lead acid battery (Figure 2.7) [9] is shown to be a mirror image of the SOC graph. If you disregard the ends of the graph where it is exponential, the graph appears to be linear which is easier to monitor and regulate its charging.

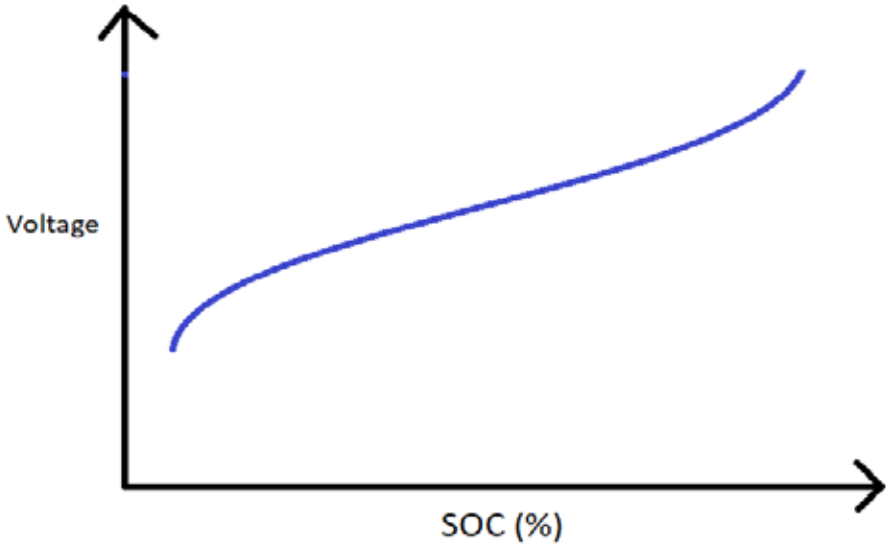

Figure 2.6 : SOC of lead acid batteries graph

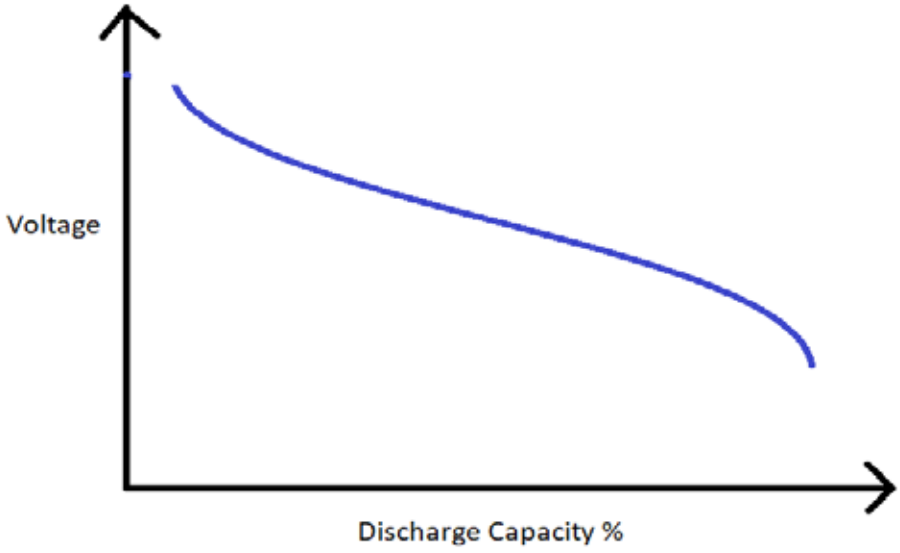

Figure 2.7 : Lead acid battery voltage vs. discharge capacity % graph

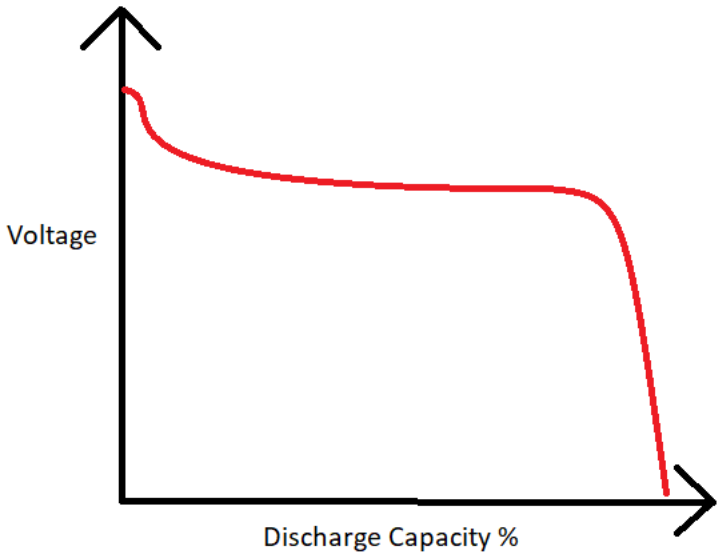

Figure 2.8 : Lithium ion voltage vs. discharge capacity graph

From Figure 2.7, you see the voltage decreases linearly as the discharge percentage of the lead acid battery increases. In contrast, Figure 2.8 shows that a lithium ion battery stays rather constant until it almost reaches the full percentage of the discharge percentage [10]. When it reaches the end, the voltage drops abruptly until it almost reaches zero. These graphs show how lithium ion batteries are better because the voltage is more consistent when compared to lead acid batteries. However, most renewable generating systems use lead acid batteries because they are lower cost and work well enough in the linear region.

2.5 Charge Controllers

One of the next most important parts of a renewable generating system is the charge controller. The charge controller is a device that takes in the power being generated by your renewable generators and stores the power into a battery bank. However, a battery bank can only hold so much charge, which is why the charge controller also monitors the charge levels of the battery bank allowing the charge controller to have the ability to supply power, when needed,

and stop the flow of power when it is not needed. Even some charge controller can data log the amount of current and voltage that is being supplied to the controller from the renewable generators, as well as, the current and voltage being supplied to the battery bank.

There are several different types of charge controllers on the market, and the one used in this thesis is the Maximum Power Point Tracking (MPPT) charge controller [11]. MPPT controllers keep the adjust the voltage going to the battery bank to seek the maximum power point. These controllers can handle varying power being received by the renewable generators because of the controller's ability to vary the voltage to current ratio while charging the battery banks. The charge controller can find the point the generator produces the maximum power and is beneficial because batteries recharge more efficiently when the charging voltage stays the same.

2.6 Inverters

The last component of a renewable power generating system is the inverter. Inverters are used to convert the DC power that is being generated and stored to AC power and is needed because most power load devices found in the common home use AC power. The inverter works by having two coils wrap around two separate ends of a metal circle or square [12]. Figures 2.9 and 2.10, show that coil 1 is connected to a switch that does not just turn the power on and off but reverses the polarity of the power. Meaning, you have a mode when normal power flows from positive to negative (Figure 2.9) and in the second mode from negative to positive (Figure 2.10). A square wave signal is created that has both a positive and negative peak. Repeated oscillations very quickly create a frequency of 60 Hz. Coil 2 receives oscillating power and discharges AC power.

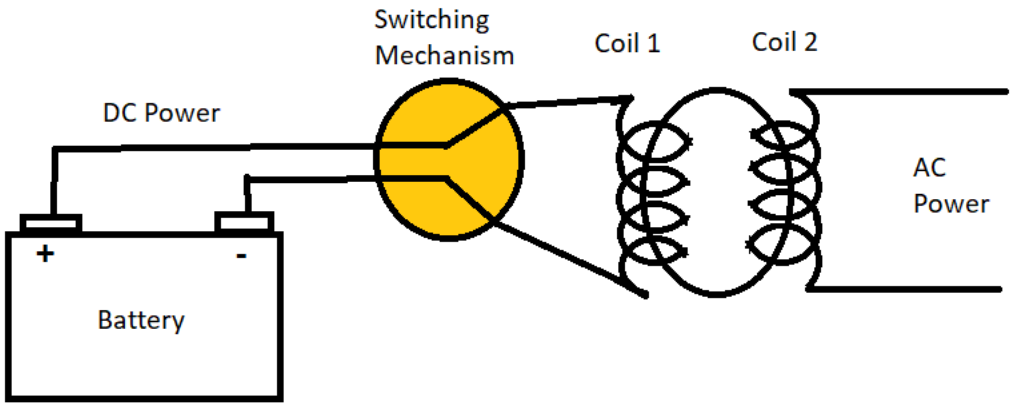

Figure 2.9 : Inverter positive to negative power flow

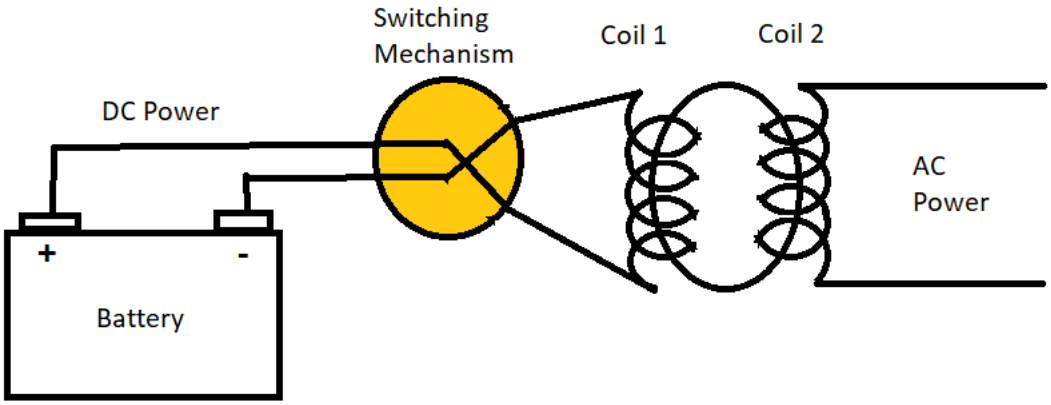

Figure 2.10 : Inverter negative to positive power flow

CHAPTER 3

MICROGRID PHYSICAL MODEL

3.1 Introduction

Chapter 2 showed the different components used to comprise a single renewable generating building. However, generators should be well maintained to work properly. In other research papers pertaining to microgrids, results show how the microgrid was very reliable [13] compared to a single renewable generating building. However, their models are comprised of many loads with one battery bank and one renewable generating node allowing many loads to be powered by one node to generate all the power for the microgrid [14]. These research papers mainly show how microgrids are more reliable and have better power quality compared to a single source, single load system.

The focus of this thesis was to simulate and build a resilient microgrid. To make a resilient microgrid, multiple buildings or nodes must be able to access multiple renewable generating sources. By configuring the nodes to connect to multiple generating sources one can access power whenever different energy sources are disconnected from the microgrid, which could be the main power grid or separate renewable generators connected to the microgrid [15]. As a result, having multiple energy sources would be valuable in areas that are prone to catastrophic events. When an area was damaged by a natural disaster, such as earthquakes and hurricanes, it has the infrastructure to supply power to its nodes.

Chapter 3 will also go over different aspects of the physical microgrid model. Section 3.2 comprises of the physical components used and their function in the microgrid. Section 3.3 comprises of the layout of the microgrid site. Section 3.4 comprises of the mounting system for the microgrid solar panel array. Section 3.5 comprises of the wiring diagram of the physical

microgrid model, and section 3.6 comprises of the expenses associated with the microgrid model creation.

3.2 Physical Components of Microgrid Model

3.2.1 Talesun TP672P-320 Photovoltaic Panel

The Talesun TP672P-320 (Figure 3.1) was the primary solar panel and power source of two house modules. For each of the house modules, four panels will be used in series. Each of the panels are tested for 36.5V, 8.77A, 320W under ideal conditions and are their maximum output. Each of the panels are composed of 72 Polycrystalline cells and are arranged in a 6 by 12 manner. During operation, the panel has a temperature range of -40 °C to 85 °C, greater or equal to 100M resistance, and a static load of 5400Pa. This creates an ideal condition 1280W of total power for each of the house modules.

Figure 3.1 : Talesun TP672P-320 solar panel

3.2.2 Crown CR-GC150 Deep Cycle Batteries

The Crown CR-GC150 Deep Cycle Battery (Figure 3.2) was used to store excess power that was generated by the solar panels and the windmill. The batteries are lead-acid that have a voltage of 12V, 150Ah, operating temperature range of -40 °C to 120 °F, and an internal resistance of 8.4m. These batteries will be oriented in series and parallel to acquire the desired voltage and power capacity for the three microgrid nodes. The two small nodes in the microgrid model will have two batteries in series making those battery banks have a voltage of 24V and 150 Ah storages. For the one large node, there will be six batteries total with two sets of three in parallel, then connected in series which creates a battery bank of 24V with a storage capacity of 450 Ah.

Figure 3.2 : Crown CR-GC150 deep cycle battery

3.2.3 Morningstar TriStar MPPT Solar Charge Controller

The Morningstar TriStar MPPT Solar Charge Controller (Figure 3.3) was the charge controller used to store the power from the solar panels to the battery bank for the three house

modules. The modules for the microgrid used the TS-MPPT-60 that can operate with the specifics of 24V, 1600W of max power. The MPPT charge controller system is composed of 4 stages. The stages are; bulk, absorption, float, and equalize. Each are used for different operating zones for the charging of the battery bank. Using this charge controller, you can also monitor the temperature, voltage, power, and current of the solar panels and battery bank. This is accomplished by connecting the charge controller to the internet or computer using the controller's Ethernet port.

Figure 3.3 : Morningstar TriStar MPPT solar charge controller

3.2.4 Solar Panel Mounts

For the solar panels to be useful for the microgrid, they best be mounted on a metal frame for stability (Figure 3.4). It was decided to use two rows of 14 feet, 1 ¼ inch galvanized pipe.

The first row was the tallest row with three 60 inches of 1 ¼ inch galvanized pipe as leg posts. The second row was the shorter row with 24 inches of 1 ¼ inch galvanized pipe as leg posts.

Figure 3.4 : Solar panel mounts

For both rows, the ends of the post were connected to the 14 feet of 1 ¼ inch galvanized pipe with 1 ¼ inch pipe elbows. The center post was connected to a 1 ¼ inch pipe tee connected to the 14 feet of 1 ¼ inch galvanized pipe after it had been halved and re-threaded. All the six posts were buried 12 inches in the ground and surrounded with concrete. After the frame for mounting was created, the panels were attached lengthwise between the pipe frames using clevis hangers. Each solar panel used four clevis hangers to mount and attach each end of the panel to the pipe frame. Using lengthwise mounting of the solar panel allowed the panels to be aligned at a 32-degree tilt; which was the optimal tilt for a solar panel in Denton, TX. The total parts used for two solar panel mounts was (8) 1 ¼ inch galvanized 90-degree elbow, (4) 1 ¼ inch galvanized

tee, (32) 1 ¼ inch clevis hangers, 105 feet of 1 ¼ inch galvanized pipe, 15 bags of 60 lb. Quikrete, and 32 bots and nuts.

3.2.5 12x16x7 Metal Shed

When creating an electrical microgrid one thing to remember was some of the electrical components are not weather resistant: the battery charge controllers, battery banks, breakers, and monitoring equipment. To keep this valuable and expensive equipment safe and dry a metal shed was purchased. The purchase of a 12x16x7 metal shed was decided on to keep the equipment safe from the weather, as well as, gave a good work area for the microgrid student to gather data. The shed was also used to house the loads used in the microgrid to simulate power usage.

3.2.6 1000-Watt Twin-Head Halogen Yellow Work Lights

The loads chosen to use in the physical microgrid model were three 1000-Watt (W) twin-head halogen yellow work lights (Figure 3.5). These lights are very convenient as loads for the microgrid because they are made from two 500W halogen light bulbs. Each light bulb can be controlled by a switch to be either on or off allowing the use of 500W for two smaller nodes and 1000W for the larger node. These wattages where chosen because the smaller nodes are composed of two solar panels and the larger node was composed of four panels. At maximum efficiency, the smaller nodes can produce 640W of power and the larger node can produce 1280W of power. Using light bulbs also has the convenience of a very stable current power draw. The stability allows testing to be more ideal for the sake of resiliency of the microgrid to supply the same amount of power to all nodes even when there are unforeseen shut downs.

Figure 3.5 : 1000W twin-head halogen yellow work light

3.2.7 Samlex PSE-24125A 1250W & Samlex PST-600-24 600W Inverters

As discussed in Chapter 2 Section 6, inverters are a key part of any renewable generating system because the DC power stored in the battery banks needs to be converted to AC power, common to household loads such as the twin-halogen work lights. The two different inverters chosen for the physical microgrid model are the Samlex PSE-24125A 1250W & Samlex PST-600-24 600W inverters (Figure 3.6). These two inverters can invert a 24 V DC power source into a 120 V, 60 Hz modified sine wave for the 1250W inverter and 120 V, 60 Hz pure sine wave for the 600W inverter. In our physical model, 600W inverters were used for the small nodes and one 1250W inverter for the large node.

Figure 3.6 : Samlex power 600W & 1250W inverters

3.2.8 Miscellaneous

Selection of wire was an important part of designing and building the microgrid. Wires are veins of the microgrid, which allow the current and power flow from component to component. Depending on the size of American Wire Gauge (AWG) conductor, a different amount of current can be transmitted safely. Using some of the wire gauge charts on the internet [16], 6 AWG can transmit up to 70 Amps (A) and 4 AWG can transmit 90A. When building the microgrid a 6 AWG was used from the solar panel nodes to the microgrid combiner box because the maximum amount of current produced by a single node was 40A. From the microgrid's combiner-box to the individual charge controllers, battery banks, and inverters 4 AWG was used. Therefore, the microgrid combiner box could output a maximum of 80A of power, 4 AWG was used. After the wire, there were a few smaller things used to make the microgrid. They were surge protectors, combiner boxes, breakers, grounding rods, nuts, bolts, washers, caps, battery connectors, and conduit. All these items seem small and insignificant, but they are all needed to make the microgrid model operational and per National Electrical Code (NEC).

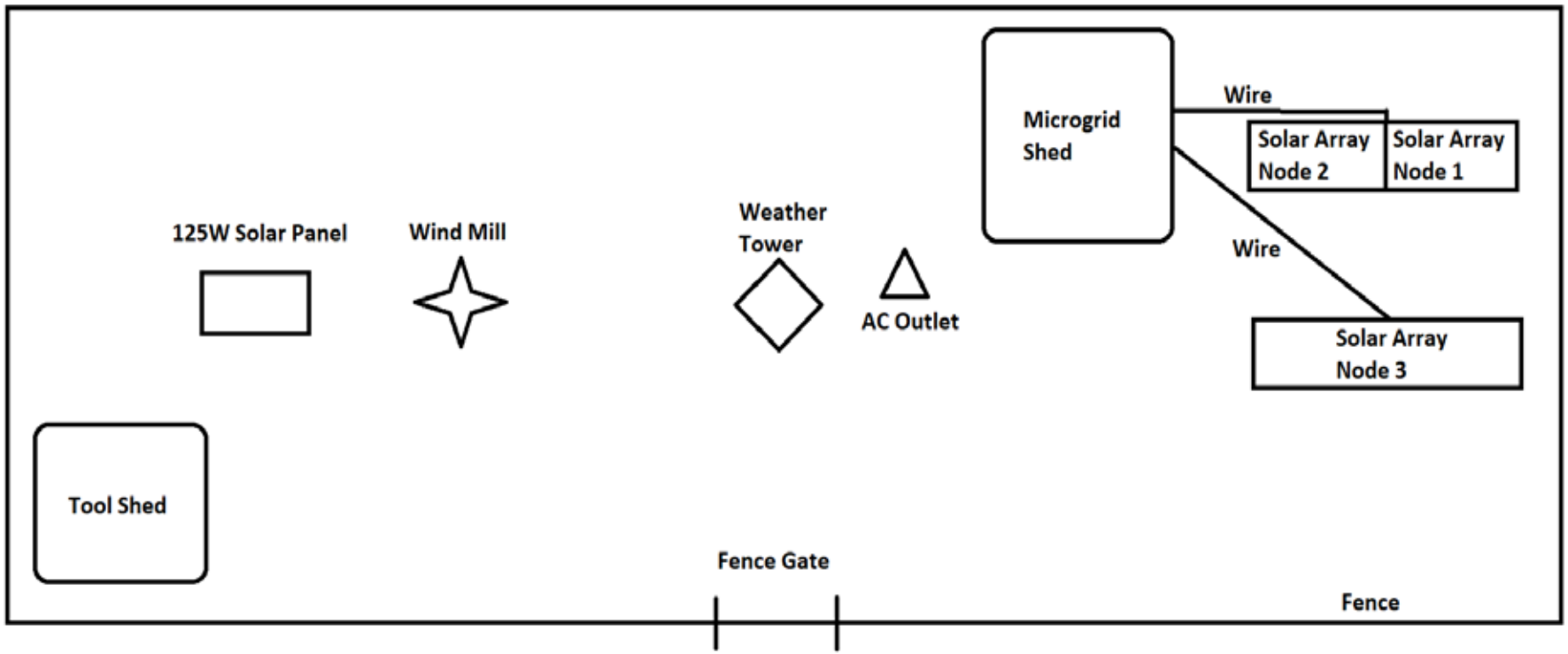

Figure 3.7 : UNT Discovery Park's microgrid site layout

3.3 Microgrid Site Layout

This section shows a layout of the microgrid site at UNT's Discovery Park created in Paint (Figure 3.7).

3.4 Mounting System for Microgrid's Solar Panel Array

This section shows the mounting system used to hold eight solar panels. These mounts where constructed with galvanized metal pipes and fittings. Figures 3.8 and Figures 3.9 where created by my professors' assistant Breana Smithers and shows the details about the mounting systems.

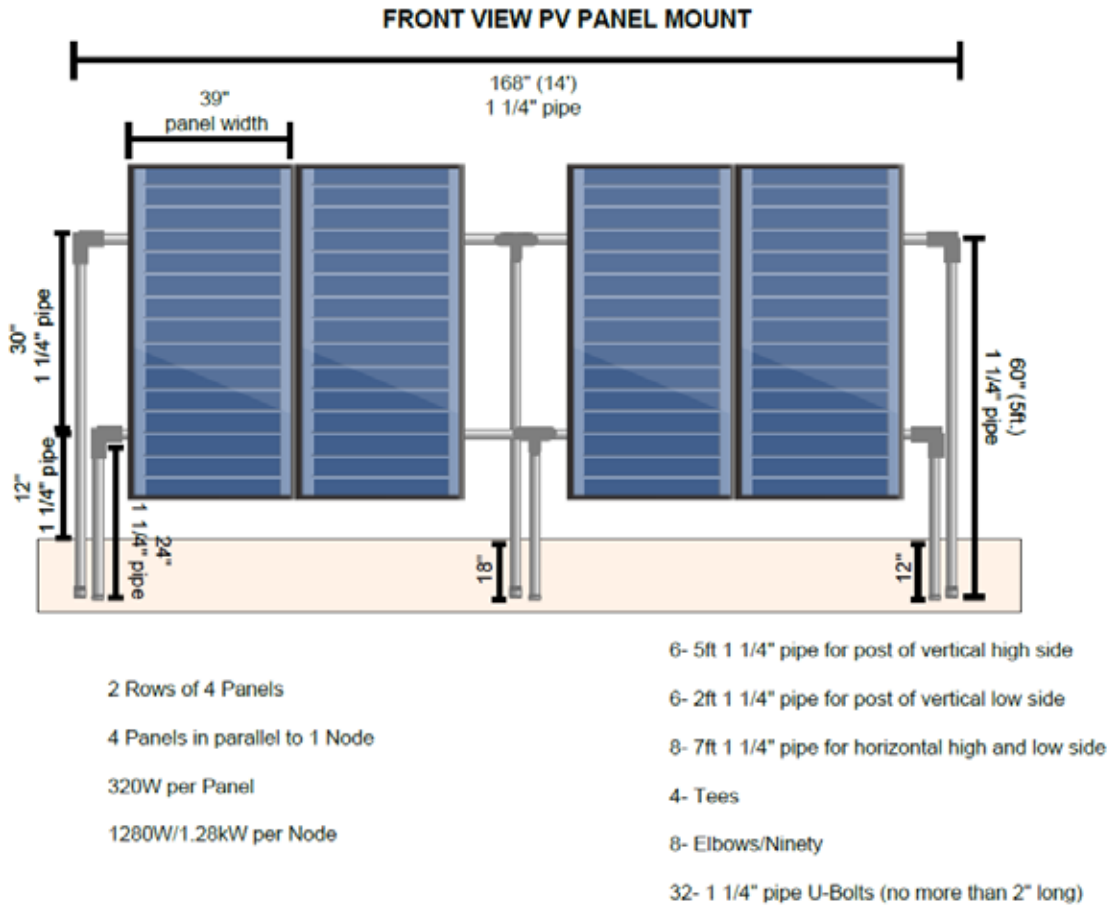

Figure 3.8 : Solar panel mounts front view (drawn by Breana Smithers)

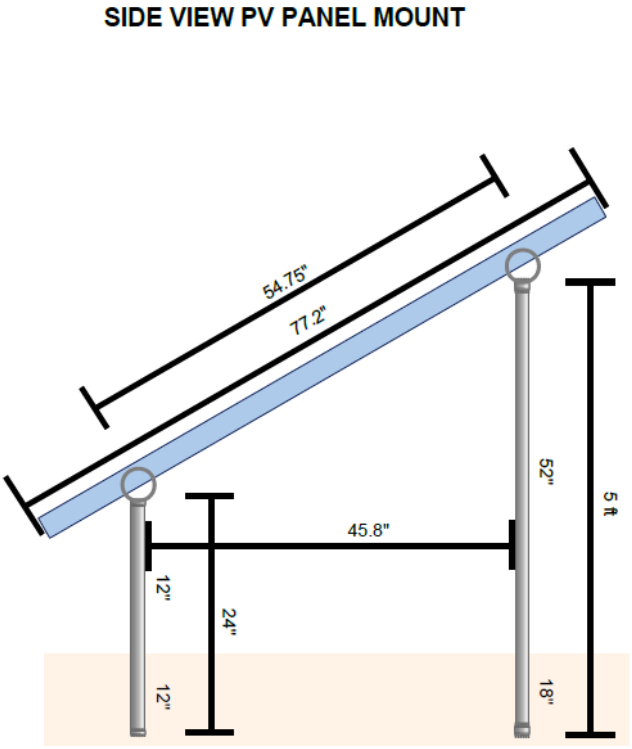

Figure 3.9 : Solar panel mounts side view (drawn by Breana Smithers)

3.5 Block and Wiring Diagrams of Microgrid Model

In this section, it is shown what the block diagram looks like for the physical model of the microgrid (Figure 3.10), as well as, the wiring diagram for the entire physical microgrid model created using LTSpice (Figure 3.11).

3.6 Microgrid Model Expenses

Section 3.6, Table 3.1, shows all the items purchased to make the microgrid model, which also shows the purchase vendor, quantity, price for one item, and total price of each item. Lastly, at the bottom the chart, the total price for all the items was added together for an easy

example of the total cost of the model minus the cost of the shed because the shed was required to house the equipment of the microgrid.

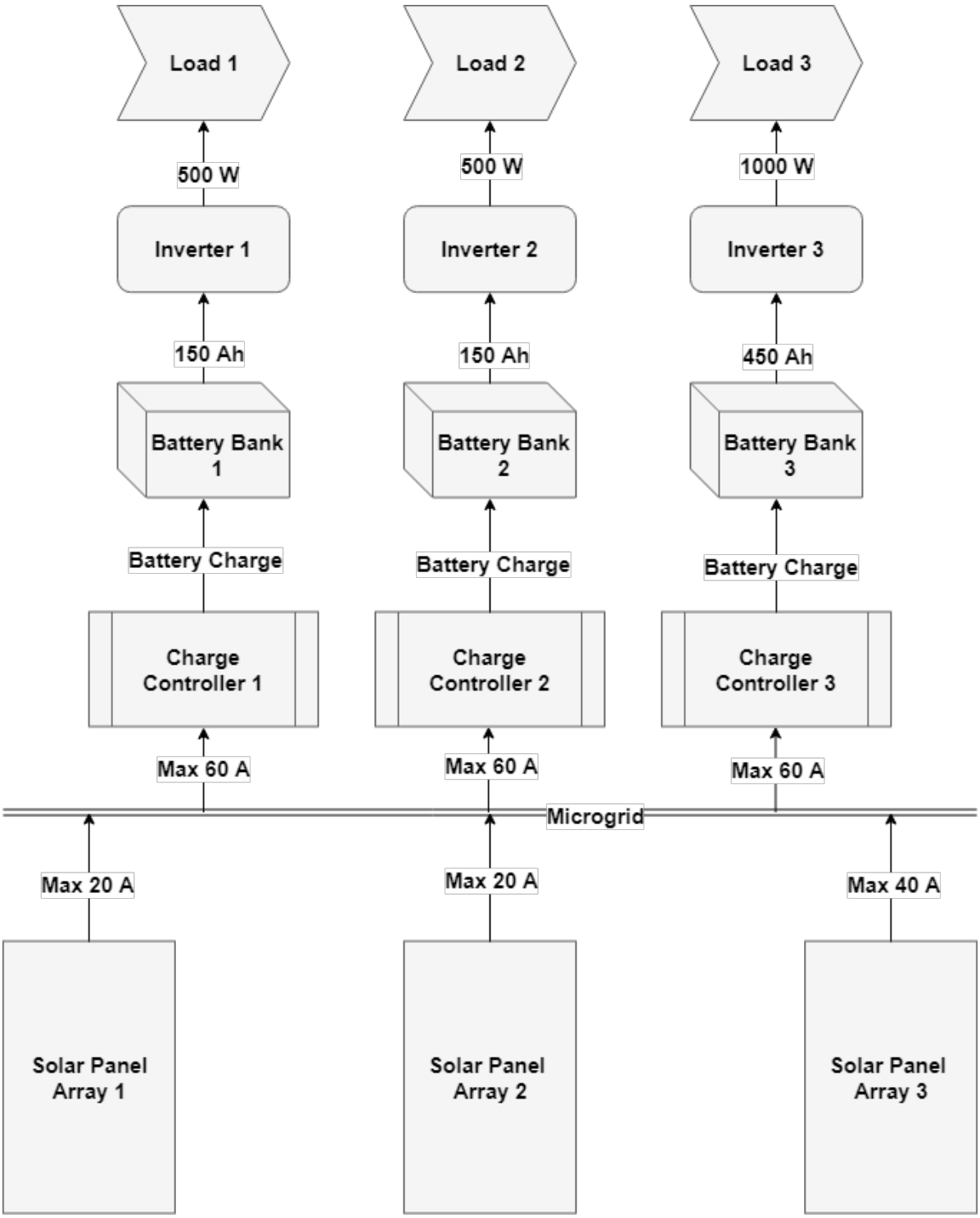

Figure 3.10 : Block diagram of physical microgrid model

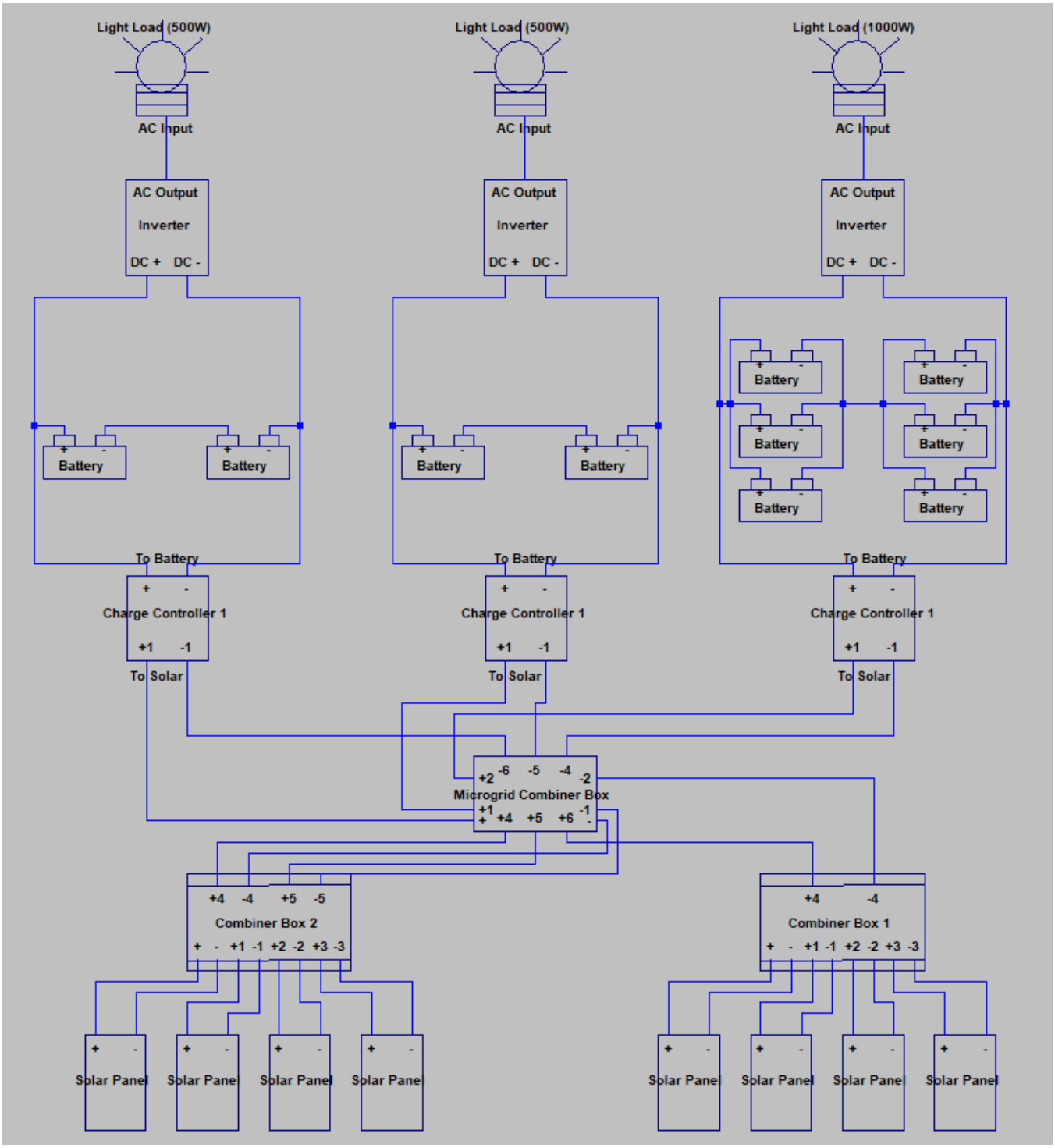

Figure 3.11 : LTSpice wiring diagram for entire microgrid model

Using the data from the simulation tool System Advisor Model, seen in Table 4.1, the average amount of money you save using a 1.28 kW solar panel array is $218 per year. For the entire

microgrid model, a combined solar production was 2.56 kW of power. From this, we can conclude that the microgrid model would save double the amount of power per year equaling $436 per year. If we then divide the total cost of the model by the amount of power saved per year, we see that it would take 20.56 years to pay back the cost of the model. Dividing $8,964.9 by the 2.56 kW of power generated, the microgrid model's cost per energy production would be $3.50 per Watt. This amount of time and cost per Watt is large because a lot of expense was used to make a small testing model. If a larger microgrid system is created the prices can be obtained more affordably because of efficiency of a larger system. Another way that the cost per year could be reduced is by investigating the amount of money saved from having a microgrid system in place during a catastrophic event. During these events, power could be lost to multiple areas and the cost of rebuilding the damaged area is very large especially without electrical equipment. Having a resilient microgrid can then save a lot of that money for reconstructing an area after a disaster.

Table 3.1 : Microgrid model expenses

Item Name	Quantity	Unit Price ($)	Total Price ($)
MidNite Solar MNPV6 Array Combiner 6 Circuit	2	88.50	177.00
PV Array Breaker 15 Amp 150 VDC	8	11.35	90.80
MidNite Solar Surge Protector	3	88.50	265.50
MC4 Female Connector Pin	12	2.50	30.00
MC4 Male Connector Pin	12	2.50	30.00
Unlocking Tool for MC4 Connectors	1	4.50	4.50
Heyco Strain Relief PV Wires	8	2.20	17.60
10 AWG Red Wire	20	0.55	11.00
10 AWG Black Wire	20	0.55	11.00
6 AWG Red Wire	100	1.89	189.00
6 AWG Black Wire	100	1.89	189.00

(table continues)

Item Name	Quantity	Unit Price ($)	Total Price ($)
TriStar MPPT Solar Charge Controller	3	550.20	1,650.60
1 ¼ Inch Galvanized 90 Degree Elbow	8	3.02	24.13
1 ¼ Inch Galvanized Tee	4	5.45	21.79
1 ¼ Inch Light Duty Clevis Hangers	32	1.90	60.75
1 ¼ Inch Galvanized Pipe	105	2.10	220.66
Talesun 320W Poly Solar Panel	8	203.97	1,631.76
Crown Group 12V 150 Ah Battery	12	171.97	2,063.64
60 LB Quikrete Concrete Mix	15	3.10	46.50
1/4 -20”x1” Hex Bolt	35	0.42	14.70
¼” Hex Nut	35	0.26	9.10
¼” Cut Washer	35	0.20	7.00
8”x16” Concrete Cap Block	2	0.95	1.90
4 AWG Black Welding Wire	100	1.69	169.00
4 AWG Red Welding Wire	100	1.69	169.00
1-inch Conduit 10 Feet	3	2.69	8.07
1 ¼-inch Conduit 10 Feet	3	5.69	17.07
Ring Terminals	32	1.25	40
MidNite Solar Array Combiner Box	1	88.50	88.50
PV 50 AMP Breaker	1	11.35	11.35
PV 30 AMP Breaker	3	11.35	34.05
Black 1 Inch Straight Cord Grip	1	4.88	4.88
Nylon Strain Relief Liquid Tight Connector	3	2.20	6.60
Samlex PSE-24125A 1250W 24VDC Modified Sine Wave Inverter	1	258.00	258.00
Samlex PST-600-24 600W 24 V DC Sine Wave Inverter	3	224.90	674.70
Allied Telesis 8 Port Switch	1	64.00	64.00
1000W Halogen Telescoping Twin Head Tripod Work Light	3	33.97	101.91
25 Ft 16/3 Extension Cord	4	8.47	33.88
Total Cost of Model	**$8,448.90**		

CHAPTER 4

SIMULATED SINGLE SYSTEM AND MICROGRID

4.1 Introduction

Section 4.1 discusses the simulation generated using Matlab's Simulink [17] and System Advisor Model (SAM) [18]. This includes a breakdown of the individual parts of the Microgrid model that was simulated in Simulink (Section 4.2), the output values from the entire model using Simulink (Section 4.3), a breakdown of a single solar generated house using SAM (Section 4.4), and the outputted graphs of the generated house using SAM (Section 4.5). These two different software programs are both valuable resources in generating data for a microgrid. Simulink allows a user to see what values you should get when certain inputs are used and what outputs you should get ideally. SAM allowed the user to see what values a single renewable generating house will use and generate. This was all useful data to compare the physical model of the microgrid to the simulation [19].

4.2 Simulink Model Parts

4.2.1 Entire Microgrid Model Overview

Subsection 4.2.1 records an overview of the entire Simulink Microgrid model [20] which allows for the discussion of the individual parts in more depth later after knowing where the current parts of the model were located and how they are connected to one another. In Figure 4.1, the Simulink microgrid model works by keeping all the different components in parallel with each other and allows the microgrid to be very resilient against any of the solar panels, battery banks, or loads getting disconnected. The model works by first reading in the solar radiation data provided by the scenario block into the solar panel blocks.

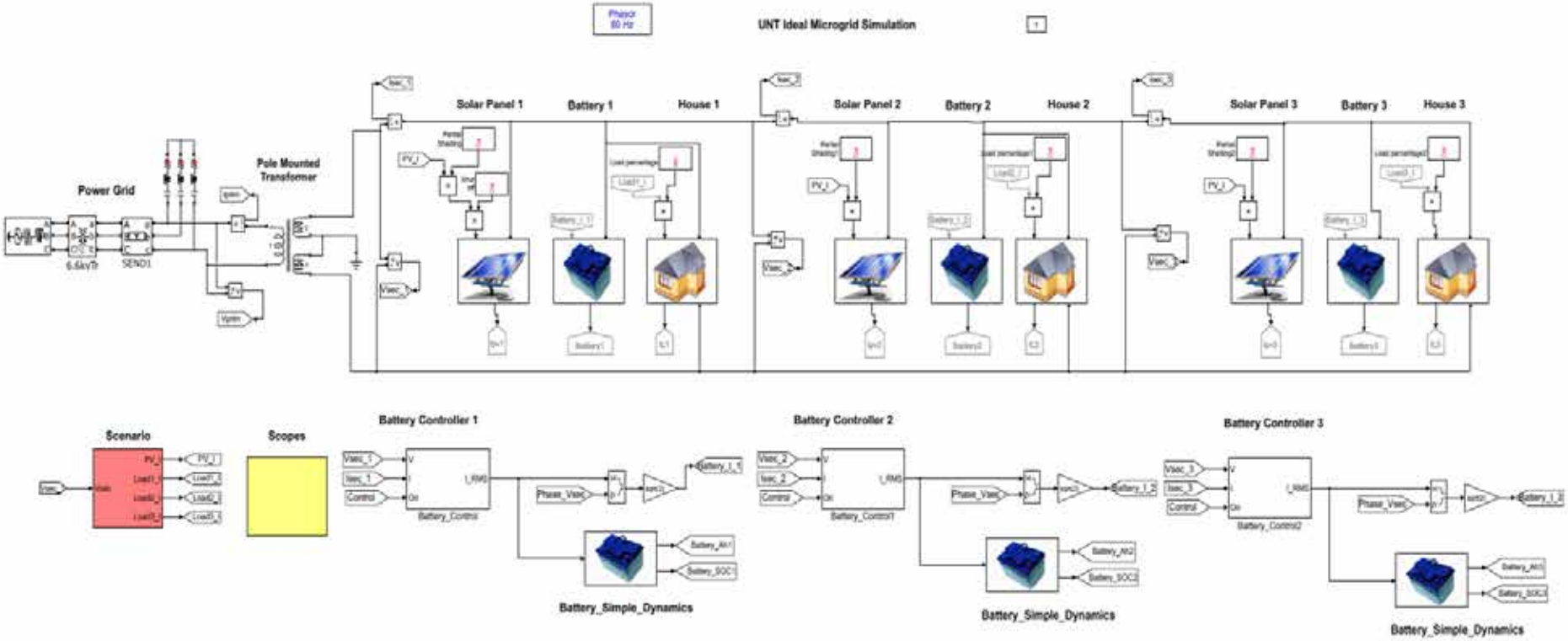

Figure 4.1 : Simulink microgrid model

The power was sent to the battery bank blocks that also send information to the charge controller blocks for the charging of the batteries. Then the power was sent to the three different load blocks that have different power requirements as specified by the scenario block. If there was any excess power, it was absorbed by the main grid. If the solar panels cannot supply enough power for the loads, then the main grid will supply the necessary power. Simulation shows 24 hours' worth of data that can then be graphed and viewed in the scope block.

4.2.2 Solar Panel

Subsection 4.2.2 discusses how the three-solar panel blocks work in the Simulink microgrid model. This was very important to the microgrid model because it simulates the three different solar panel arrays that create the physical microgrid model. As seen in Figure 4.2, the solar panel block has three different connection points. The first connection point multiplies the PV_I signal by a partial shading value, which allows the use of the solar radiation data that comes from the scenario block (PV_I) and multiply it by shading percentage. To calculate the total solar radiation, multiply the received solar radiation by one minus the shading percentage. Using this idea, a set percentage, time, and duration of shading can occur. For instance, the shading could be 10% starting at hour 11 and lasts 3600 seconds (1 hour). Then put 0.9 in the value section of the partial shading function, starting at 11 hours and lasting for 3600 seconds.

The second connection point transfers the power generated in the circuitry of the solar panel block into the microgrid, and the third connection point outputs the current of the solar panel. The output can then be graphed in the scope block of the microgrid mode. In Figure 4.3, the user can see what the circuitry looks like for the solar panel block. The circuitry comprises of a controlled current source, a snubber resistor, current measurement, input port, output port,

physical modeling connection port (PMC Port), and a ground connection. The current source uses the data from the input port, which was connected to the PV_I data from the scenario block. The numbers generated by the scenario block become current values at an AC frequency of 60 Hz. The positive connection of the current source was connected to the current measurement source that outputs the current value to the output port, which was connected to the Ipv1 link, and was graphed in the data. The current measurement source then connects the PMC port, which sends the current generated by the solar panel block to the microgrid. Lastly, the current source's negative terminal connects to ground. However, to make sure the current flow was not too large, a snubber resistor of 1 mega ohm was used from the current sources positive to negative terminal. Which acts as a buffer to make sure the power will go straight to ground if the current gets too large.

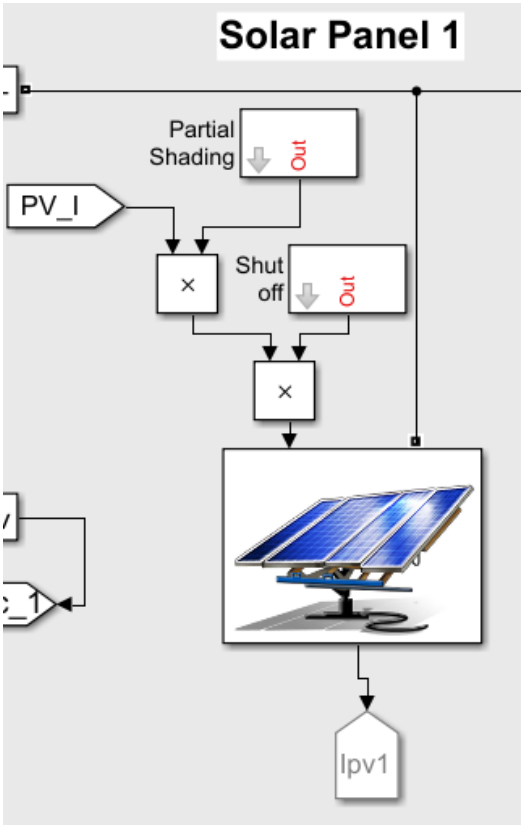

Figure 4.2 : Simulink solar panel block

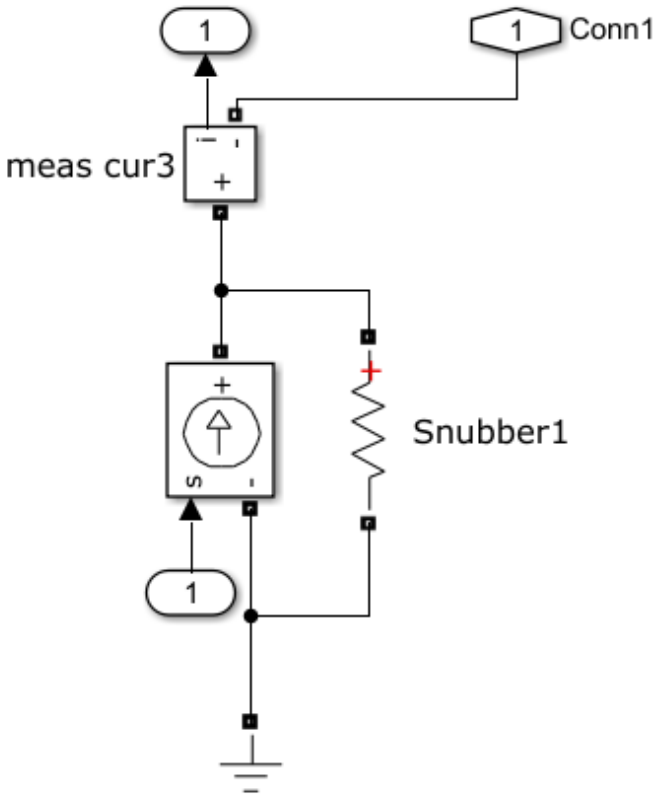

Figure 4.3 : Simulink circuitry of solar panel block

4.2.3 Battery and Battery Controller

Subsection 4.2.3 discusses how the three battery and battery controller works in the Simulink microgrid model. As seen in Figure 4.4, the battery block has three different terminals. The terminal labeled Battery_I_1 was the input current value from the battery controller block, the label Ibattery1 was the output current value from the battery, and the last terminal supplies power onto the microgrid or supplies the power to the load block. Inside the battery block, the circuitry was the same as the solar panel block seen in Figure 4.3.

Figure 4.4 : Simulink battery block

The battery block was not as interesting as the battery controller block. The battery controller block was where the values for how much power was being supplied to the battery block was located, as seen in Figure 4.5. The block first inputs Vsec_1, Isec_1, and Control values into the Battery Control block. Vsec_1 and Isec_1 are the voltage and current measured in the microgrid as supplied by the solar panel block. The Control input was a signal generated in the scenario block that works like a PWM signal for the controller. The circuitry inside of the Battery Control block was shown in Figure 4.6. The Battery Control block works by using the Vsec_1 and Isec_1 values and passes them threw an Active & Reactive Power phasor expression. From there the values that are generated are passed into a switch with a threshold of 0.5 using the values from the Control input signal to flip flop from the power signal that was created before to zero. The switch value was then added to the previous value from the Active & Reactive Power phasor expression and was passed through an expression that multiplies the

signal with a gain of 0.1. The new signal was then integrated with the original Control signal to generate the I_RMS value for the Battery Control block. Briefly, the battery controller converts an AC signal to DC and restrains the amount of power absorbed by the microgrid.

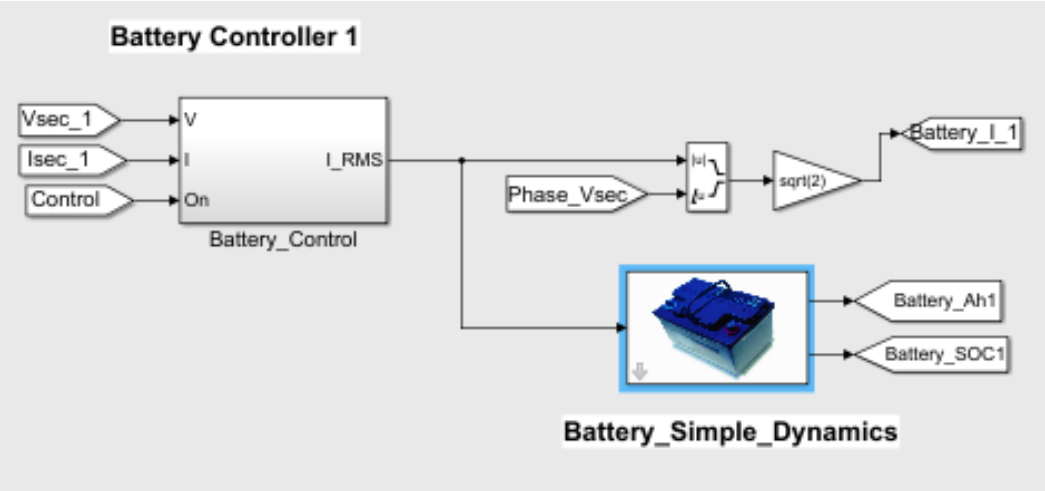

Figure 4.5 : Simulink battery controller block

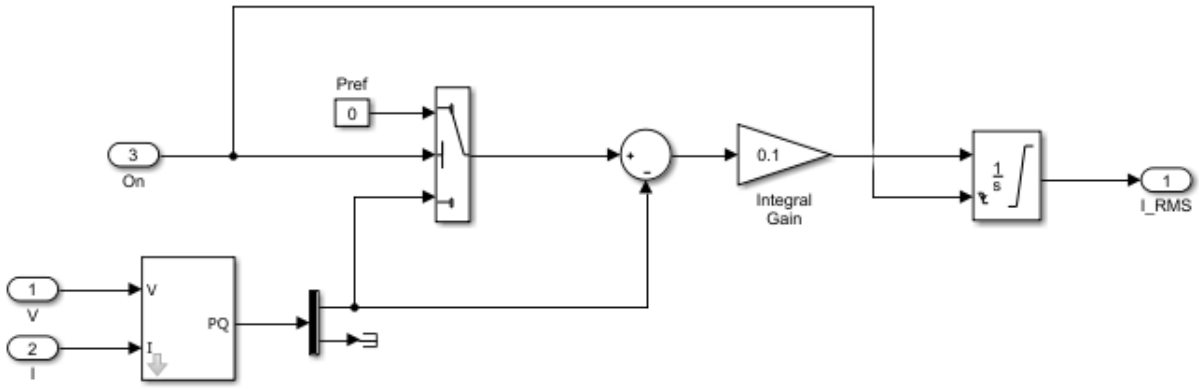

Figure 4.6 : Simulink circuitry of Battery Control block

The I_RMS value was then passed to a Magnitude and Angle expression that creates a new output signal that was multiplied with a gain of square root of two, then the value was passed to the battery block, as seen in Figure 4.5. The process converts the DC power signal back into AC power so to be consistent with the AC power being used by the microgrid. The I_RMS value was also passed to a battery subsystem expression of a 1000 Ah, which can be changed,

with the size of your battery banks. The battery subsystem then outputs two values called Battery_Ah1 and Battery_SOC1. These two values were graphed using the scope block to show the battery's Amp-hours with respect to time and the battery's State of Charge (SOC) with respect to time.

4.2.4 Loads

Subsection 4.2.4 discusses how the three Load blocks work in the Simulink microgrid model. The load blocks in the microgrid, as seen in Figure 4.7, are comprised of the house block with one input and three output terminals. The one input terminal works by reading the load values in Load1_I from the scenario block. From there the value from Load1_I was multiplied by a percentage from the Load Percentage expression. The load percentage expression may be given any numerical value at any given time and length during Simulink's simulation allowing the user to add a percentage and adjust the value being multiplied by Load1_I. For instance, if you want the house to have increased current compared to the other two houses you can multiply the same Load1_I by 1.2 increasing the load by 120% for the specified time and length.

The three different output terminals at the load block serve different purposes. The first output sends the current value of the load (IL1) to the scopes block for measurements. The other two outputs receive the required current from the microgrid for the loads to use power. Inside of the house block there was a circuit as seen in Figure 4.8. This circuit was as the circuit found in Figure 4.3; however, the block act as a load instead of a power source. At the top of the circuit, there is a resistor of 16 ohms to simulate some minor power loss from wires. The main difference between Figure 4.8 and 4.3 is the negate terminal of the current source and snubber resistor are connected to the negative terminal of the microgrid instead of ground which allows the current

source to generate negative power output instead of positive power output as seen in Figure 4.3. The negative power was then added to the power being shared in the microgrid model. It simulates a subtraction in power from the microgrid which keeps the model's AC power frequencies the same and subtracts power from the microgrid at the same time. Of course, assuming a perfect microgrid with no interference or noise.

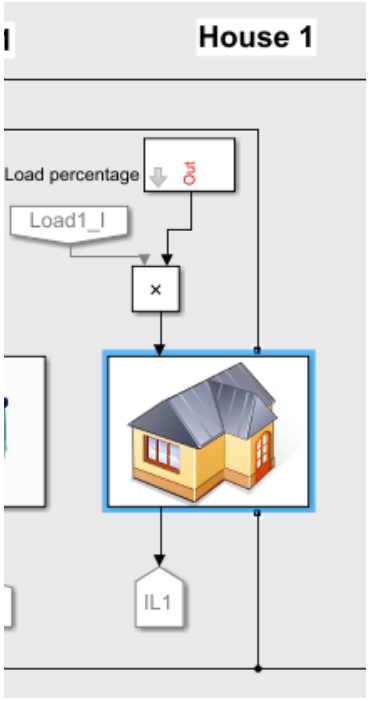

Figure 4.7 : Simulink load block

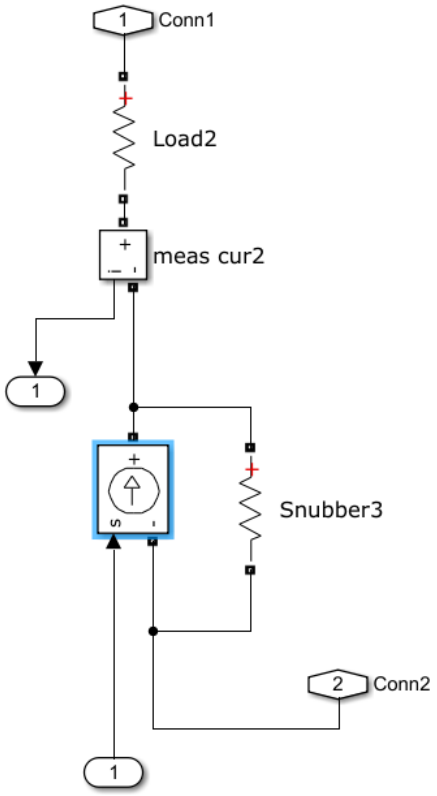

Figure 4.8 : Simulink circuitry of load block

4.2.5 Grid

How the main grid block of the Simulink microgrid works is described in subsection 4.2.5. The main grid block part of the microgrid is also important as it shows how the main grid can both supply and absorb power from the microgrid. The main power grid block as seen in Figure 4.9, works by a circuit comprised of a power grid section and the pole mounted

transformer section. The pole mounted transformer section works by using Simulink's linear transformer model and takes power from the power grid then steps it down in power to match the power and frequency of the microgrid, which was then connected to the power grid section. The power grid first takes the connections from the linear transformer and passes it through a three-phase transmission line model, which consists of one set of RL series elements and two shunt capacitances. Line models need to connect three series RLC loads to keep the two terminals to the linear transform model consistent with each other. The three-phase transmission line model then connects to a three-phase transformer rated for 6.6 Kilo Volts (kV). The three-phase transformer was connected to a three-phase source, which outputs a voltage of 6.6 kV at a frequency of 60 Hz. The three-phase source and three-phase transformer are what simulates the large power being supplied by the main grid from a large power plant.

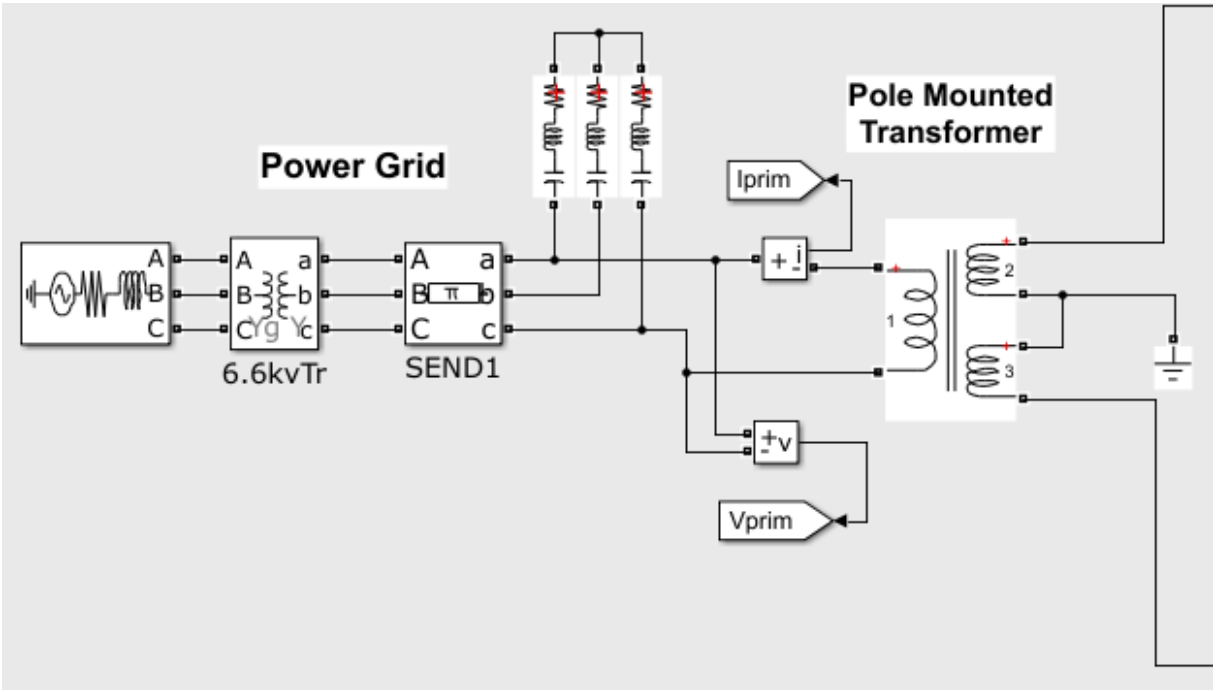

Figure 4.9 : Simulink main grid block

4.2.6 Scenario

Subsection 4.2.6 discusses how the scenario block works in the Simulink microgrid model. As seen in Figure 4.10, the scenario block has one input value and four output values. The input value Vsec_1 was the voltage value that was being read from the microgrid. The four-output values PV_I, Load1_I, Load2_I, and Load3_I are all values that were used at different blocks in the microgrid.

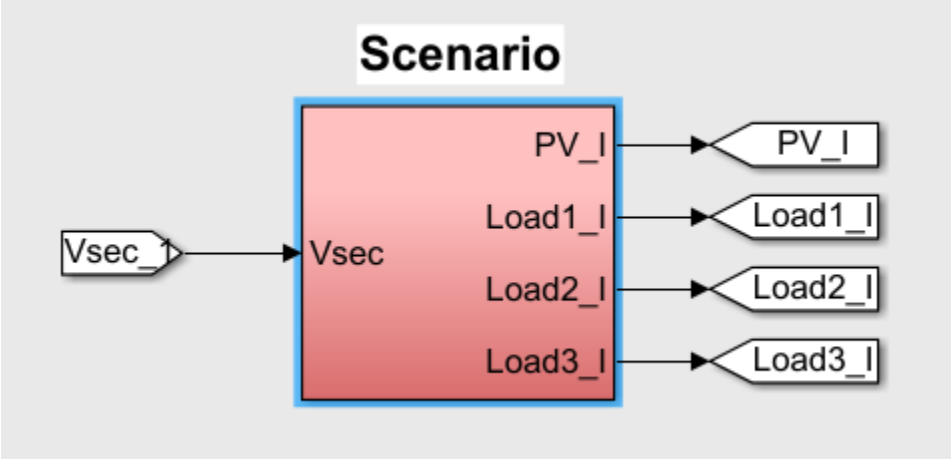

Figure 4.10 : Simulink scenario block

When looking inside of the scenario block (Figure 4.11) you will see the conditions that make the scenario block operate. The block first works by using the clock expression from Simulink to simulate the time for each decimation of the simulation of 24 hours. The time was then split up evenly into the Load Data 1-D Lookup Table and the Solar Data 1-D Lookup Table. These two expressions stored the load data of a normal house with a peak load of 2500W and the solar data for a 5-kilowatt array of solar panels in the span of 24 hours. The load data was multiplied by a factor of 0.4 to gain the load data of a normal house with a peak load of 1000W. The value was then multiplied by a gain of 1/200 and -1 so to simulate a negative number of current. The solar data was multiplied by the constant 0.25 to create a solar array closely relating to 1.28-kilowatts and was multiplied by a gain of 1/200 but stays positive to simulate positive

current. The two arrays of numbers were combined with at mux and multiplied with the gain of square root of 2 and created the magnitude of the solar and load data. Input terminal Vsec was used to take the angle or phase of the voltage from the microgrid. The angle and two magnitude values were passed through a magnitude-angle block to make two new arrays of values with both having matching angles. These arrays were then de-muxed to have the three load values Load1_I, Load2_I, and Load3_I that were matching values, and the PV_I value for the current of the solar panel array.

The last thing generated in the scenario block was the output signal “Control” to create a PWM signal for the battery charge controllers by adding two square wave functions together called Step_Off and Step_On. The two square waves are different by Step_Off having at step time of 12*60*60, initial value of 0, and final value of 1. Step_On however, has the step time of 18*60*60, initial value of 0, and final value of -1. Once added together, the new square wave passed through a switch, which alternated from 0 to 1 depending on the positive or negate signal from the old square wave created the “Control” signal used by the battery charge controller.

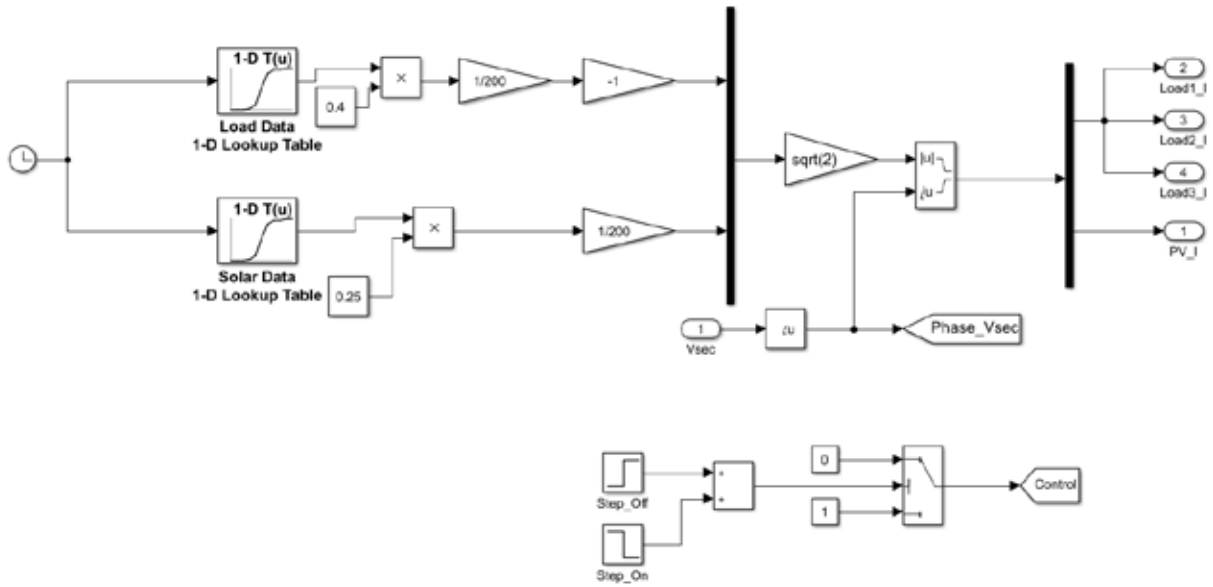

Figure 4.11 : Simulink conditions of the scenario block

4.3 Simulink Model Results

Using the Simulink model, mentioned in the previous sections, one can generate some interesting results given the necessary input variables. The model comprises of a Main Grid, three loads, three battery charge controllers, three battery banks and three solar panel arrays. To make the simulation like the physical model of the microgrid, the input variables were constrained. For House 1 and 2, the load values did not exceed 500W. Solar panels 1 and 2 produced a max of 625W and battery banks 1 and 2 were 150 Ah making the two modules in the Simulink microgrid like the two small nodes in the physical model microgrid. House 3 had a max load value of 1000W, Solar panels 3 produced a max of 1250W, and battery bank 3 was 450 Ah, simulating the large node in the physical microgrid model.

Running the simulation for 24 hours created the following graphs in the scope section of the Simulink microgrid model. Figure 4.12 shows the Power_PV Panels 1, Power_Secondary (aka. Power on Microgrid), Power_Load 1, Power_Battery 1, Battery_SOC 1, and Time in Hours. Figures 4.13 and Figure 4.14, showed the same graphed values but for module 2 and 3 respectfully.

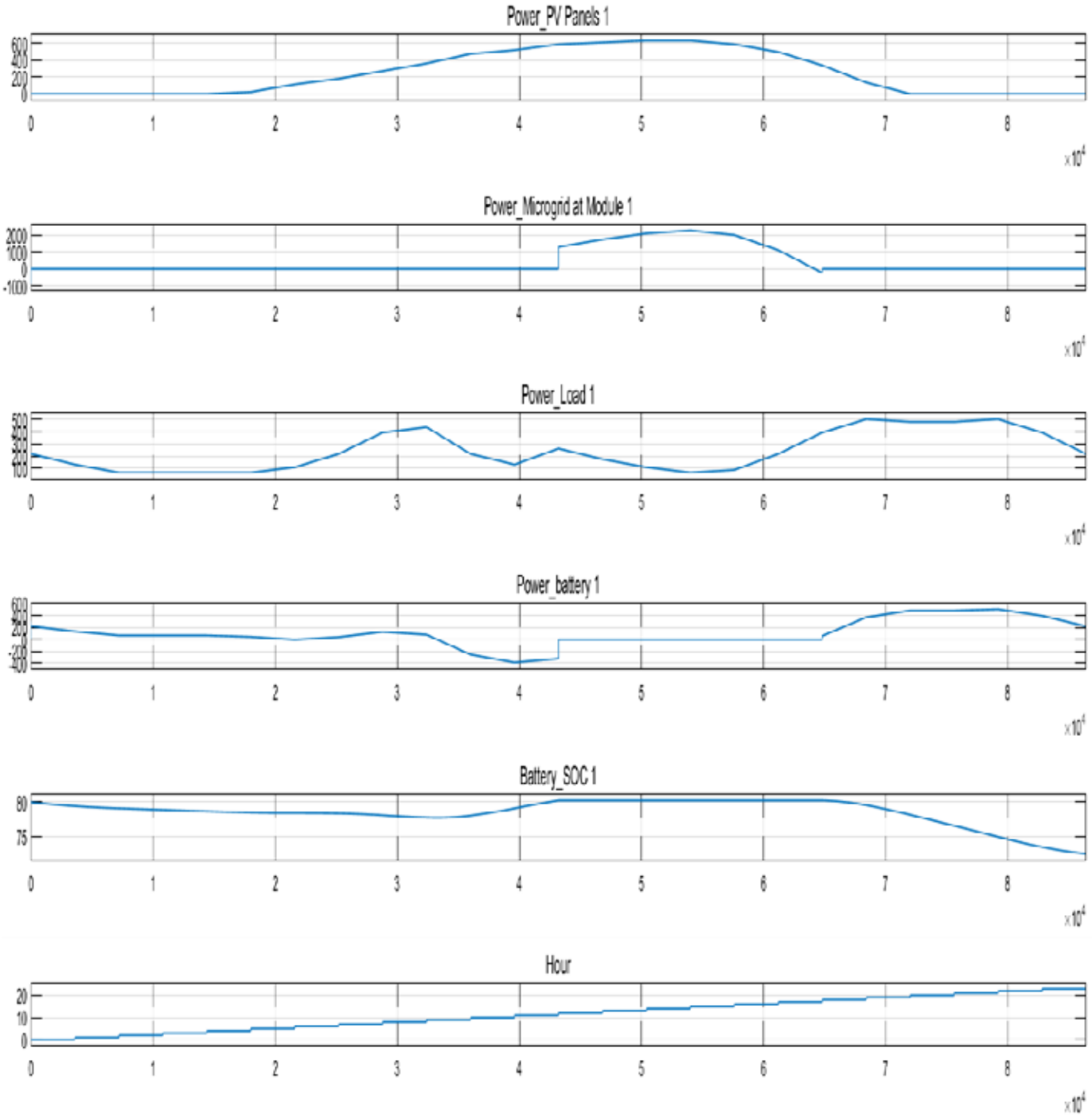

Figure 4.12 : Simulink module 1 output graphs (normal operation)

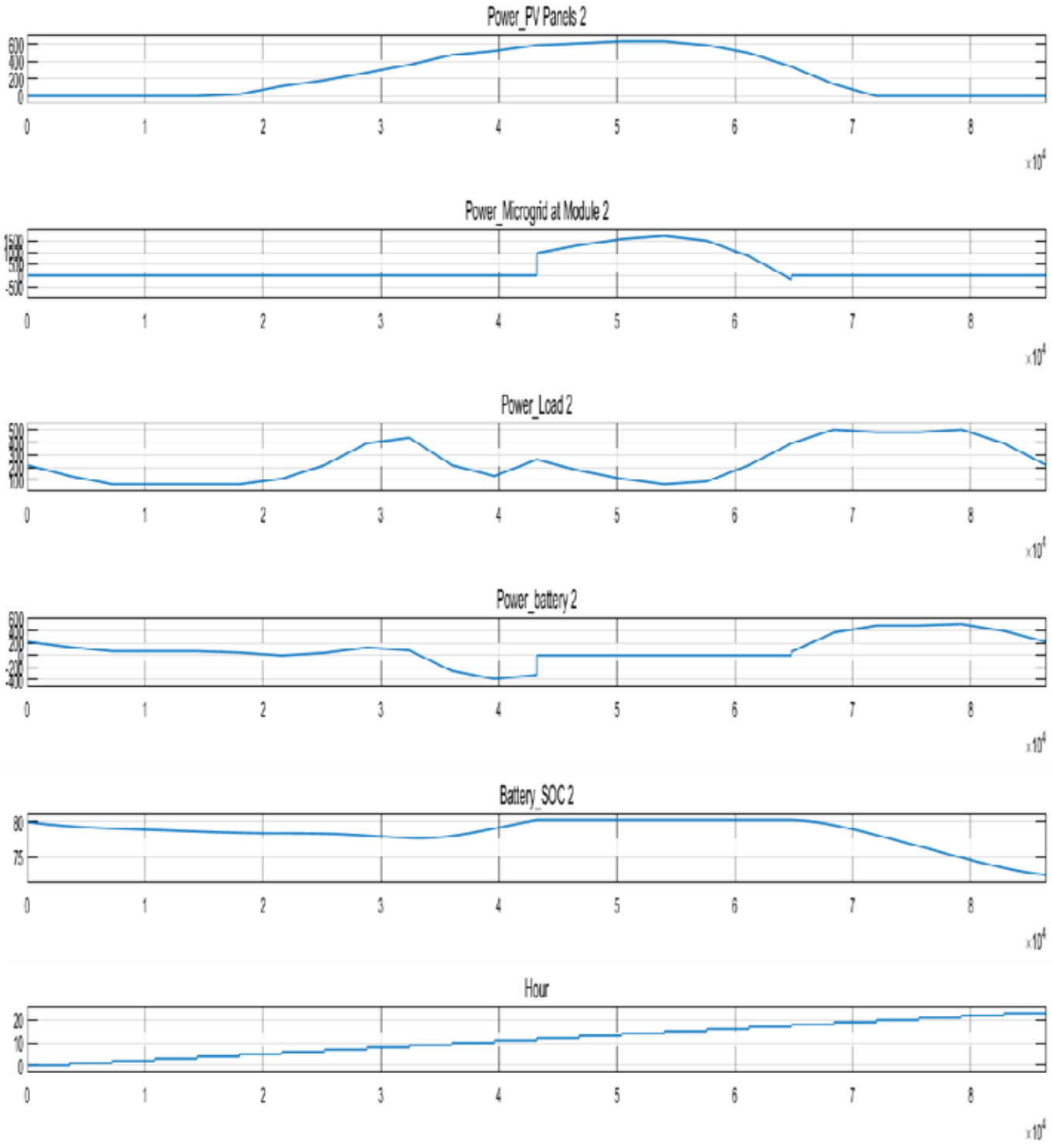

Figure 4.13 : Simulink module 2 output graphs (normal operation)

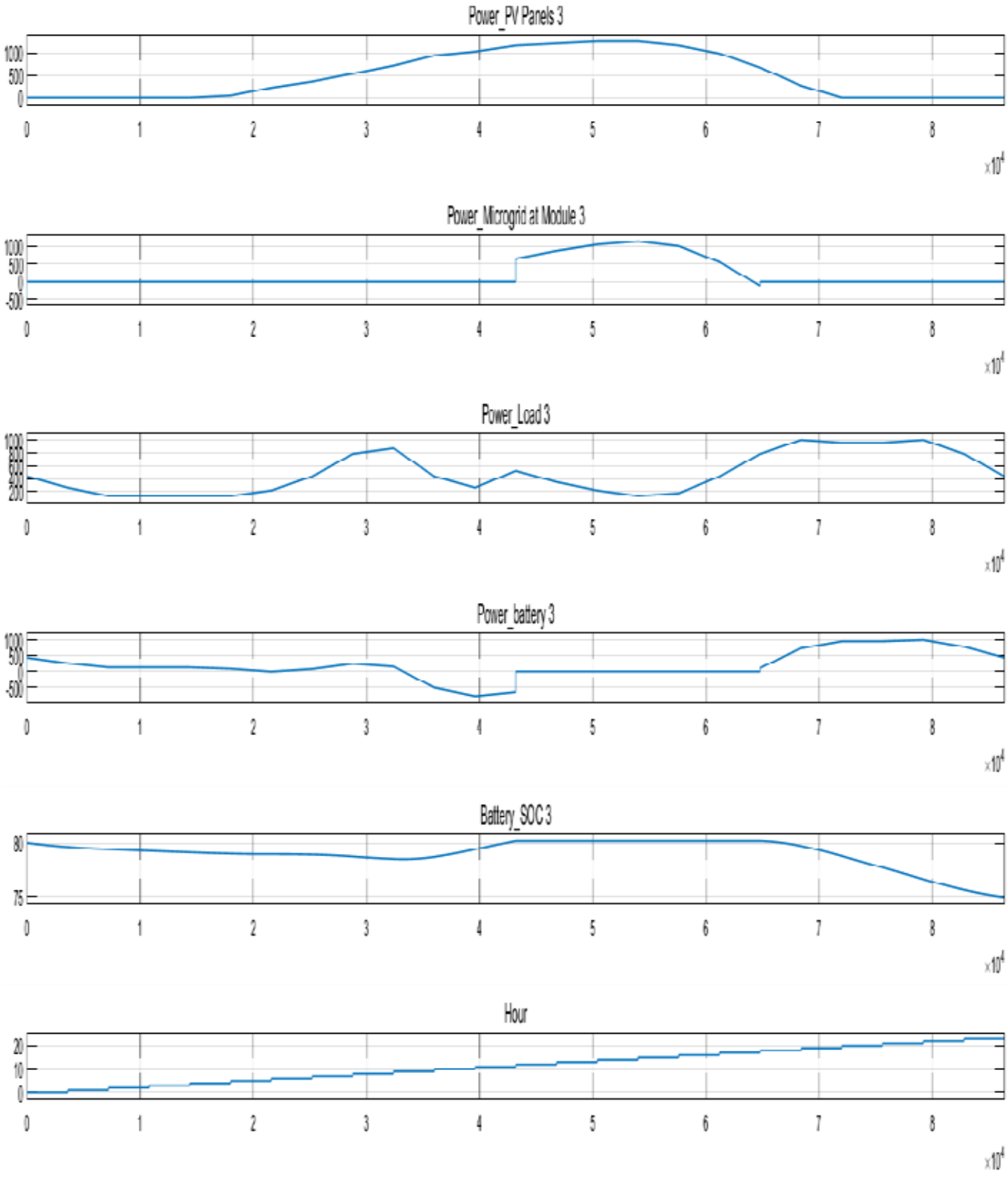

Figure 4.14 : Simulink module 3 output graphs (normal operation)

From Figures 4.12 – 4.14, it was seen that using these input constraints the microgrid operated effectively without ever needing to absorb power from the main grid. The Power Secondary graph shows where the power on the microgrid was zero until the amount of power generated by the panels and stored in the battery banks was sufficient to power the loads. Once this occurred, excess power was supplied to the microgrid for other nodes to absorb power or for the main grid to absorb.

Figures 4.12 – 4.14 show the benefits of a microgrid. However, for this paper, a test of the resiliency of the microgrid was proven. This was done in the simulation by cutting off the PV power production for one of the modules. When this happens, the microgrid needs to be resilient enough to supply power to that module. To simulate, the power was cut off to module 1 for 7 hours, which was the small node in the physical model. Figure 4.15 shows the measured results at module 1.

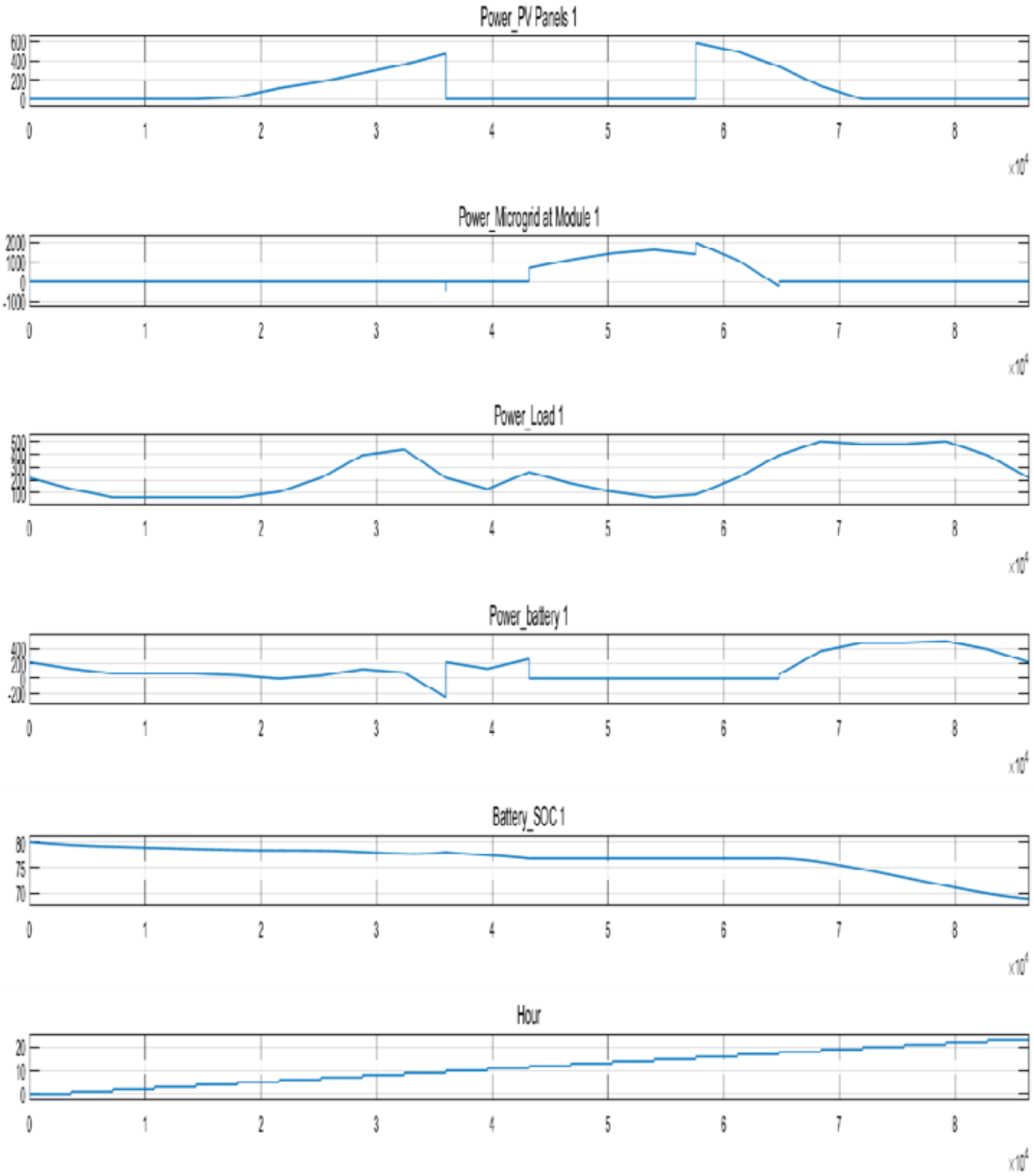

Figure 4.15 : Simulink module 1 output graph (6 hours of PV shut off time)

Figure 4.15 shows when the PV panels in module 1 were disabled for 6 hours the microgrid and battery banks supply the power to the loads that caused the batteries SOC to decrease instead of increase and the excess power in the microgrid to fall. Yet, this is to be expected and what you want to see in a resilient microgrid because the excess power in the microgrid was able to supply power to the loads during a sudden power supply shut down. A sudden power supply shut down can be caused by a multitude of reasons but the most common would be a natural disaster.

4.4 SAM's Breakdown for a House

Using the software System Advisor Model (SAM), a user can gain very useful information about how renewable generating system can save a user money. SAM software works by taking the specifics about a renewable generating system and generates charts and graphs about its theoretical operation. The SAM software has limitations of not being able to simulate a microgrid. However, using the software shows useful information about how a single module works in a microgrid it will comprise of solar panels, inverters, batteries, and loads.

To understand what the outputs of the SAM simulation are, let us look at the specifics of the software. First, when creating a new project in SAM, one needs to know the specifics of the hardware. Which could include the model number of the solar panels, batteries, and geographical location of the site. Once all the specifics are known, one can start putting in data to the SAM software. The software starts with the geographical location of sight. The software makes it easy because SAM can look at an online database for the specifics of the area. Once the site location was entered, the software downloads the specifics for a region. SAM then automatically fills in most of the blank specifics for the solar radiation for a region.

From there, then move to the module section of the SAM software where one can investigate a database full of different solar panel brands and models. Once the panel was selected, the data was then filled in for the specifics of the solar panels including current vs voltage curve, temperature specifics of the panel and area the panels occupy. Next, the inverter model used for the simulation was selected. The software then filled in the efficiency vs rated output power for the inverter.

Once the system was designed, the SAM software filled in most of the empty boxes because of the solar panels chosen earlier. However, there were a few more things needed. A designated array size and DC to AC ratio for the system need was added. In this case, 1.2 kWdc was chosen and a DC to AC ratio of 1.20. Next, the positioning of the solar panels was selected and set up for fixed, seasonal tilt, azimuth axis, etc. The solar panels were mounted in a fixed position of 36 degrees of tilt, with an azimuth degree of 180, and ground coverage ratio of 0.3.

The next part of the SAM software covers the shading and snow that could cover a solar panel. In the simulation, it was kept at zero so that the outputs will be their absolute max efficiency. SAM then allows the user to input different loss parameters in the simulation model. It is useful if the percentage of lose expected was known going from component to component. Losses were set at a minimum with a 5% loss from annual soiling, 0.5% diode and connection loss, and a 2.490% total DC power loss. The SAM software allows the user to add a value for the degradation rate for the lifetime of the renewable generating system. A 0.5% degradation every year was chosen.

The SAM software allows for the properties of the batteries to be entered and to specify the type of batteries used, the specific cells used, voltage properties, cell capacity, and other specifications. Flooded Lead Acid batteries were used; 2 cells in series with 3 in parallel, bank

voltage of 24V DC, cell nominal voltage of 2.37V DC, cell internal resistance of 0.008 Ohms, cell capacity of 450 Ah, and DC to DC efficiency of 99%. The next few sections for the SAM software involve the system cost, financial parameter and incentives. These sections allow users to designate the cost spent on the hardware of the model, finances and loans to own them and incentives, if any, given by the state or federal government for renewable energy systems. However, it was chosen to keep these blank since it was for research purposes, and the physical model discussed has more cost parameters than what SAM can provide.

The final two sections for the SAM software are called Electricity Rates and Electricity loads. Electricity rates are easily filled out because SAM allows a download of the average electricity rates for a given area online, and was the same area used earlier in the Location and Resource section. However, the difference here was choosing from various power company providers if your area offers them. This, in turn, can change your rates and change the data automatically once the power company was selected. The electric load section was then automatically filled in once the location for your electricity rates was chosen. The same field has the average monthly data usage for an area. Once all these parameters are completed, the user can then simulate the renewable generating system that was created.

4.5 SAM Output for a House

Section 4.5 output graphs, charts, and figures were generated using SAM software. From the previous section, how the individual sections of SAM were used and what values were used for one module of the Microgrid were discussed showing what kind of data to expect with just one renewable generating system being used. The single renewable generating system was with respect to the average power being generated and used in Denton, TX. Figure 4.1, shows a table

generated by SAM. The chart gives a snapshot into the key points generated using SAM. As seen from the figure, the annual energy for one year was 3,730 kWh, which means a normal house in Denton consumes about 3,730 kWh of power each year. One of the next things to note from the figure was 1,456 kWh/kW of power for an energy yield. Which means about 1,456 kWh of power could be generated from the solar panel arrays for a year. The next two things to note from the figure was the electricity bill without using the solar panel system was $452 a year. The electricity bill for the year was reduced to $233 when the solar panel system was used. The total cost savings of the solar panel system was more than half.

Table 4.1 : SAM simulation overview table

Metric	Value
Annual Energy (One Year)	3,730 kWh
Capacity Factor (One Year)	16.6%
Energy Yield (One Year)	1,456 kWh/kW
Performance Ratio (One Year)	0.70
Battery Efficiency	69.08%
Levelized COE (Nominal)	12.31 cents/kWh
Levelized COE (Real)	9.74 cents/kWh
Electricity Bill Without System (One Year)	$452
Electricity Bill with System (One Year)	$233
Net Savings with System (One Year)	$219
Net Present Value	$-1,921
Payback Period	NaN
Discounted Payback Period	NaN
Net Capital Cost	$10,790
Equity	$0
Debt	$10,790

Another thing generated by the SAM software was the monthly energy production for the system shown in Figure 4.16 as a bar graph for each month in one year's time. As you can see from the figure, most of the power generated was in the months of July and August with

December being the lowest. It made sense because the summer days are longer and mostly clear in Denton, TX, but days in the winter are shorter and partly cloudy.

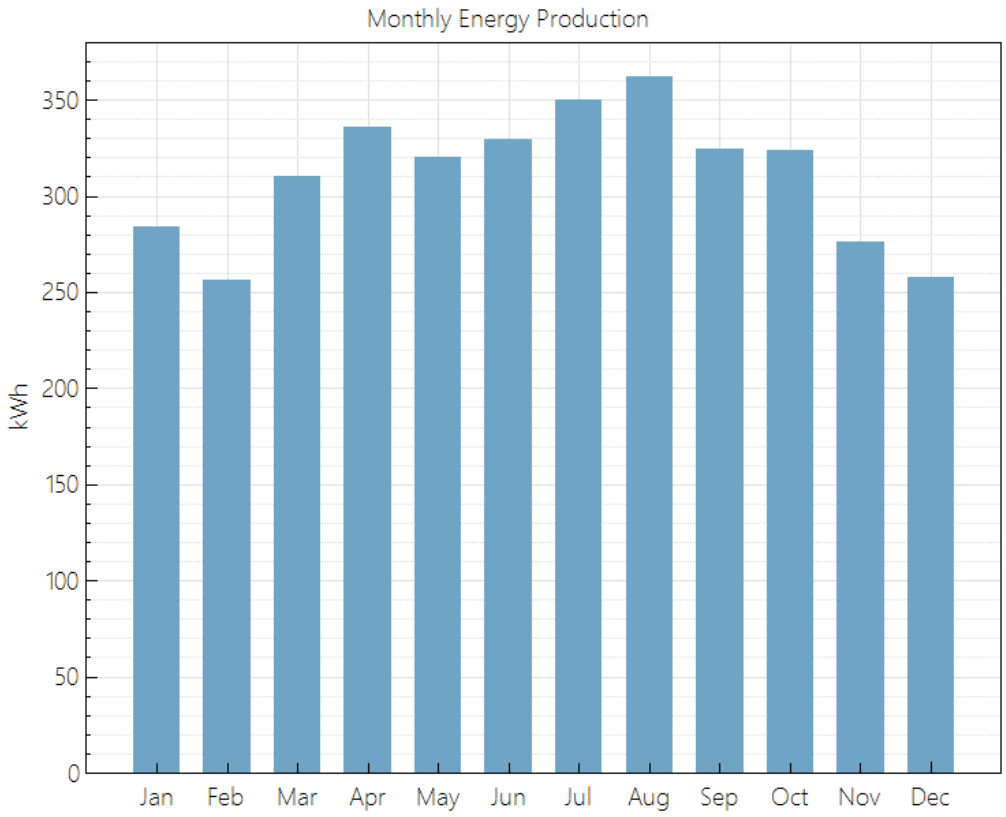

Figure 4.16 : SAM monthly energy production graph

The next graph generated in SAM was the Monthly Energy and Load in Figure 4.17 that allows the user to see what power was being generated for each month and easily see how much power was being consumed for the same month. The load was an average found in the database for houses in Denton, TX, and shows if your renewable system was generating enough power for your house or for just some of it. Not enough power was generated for all the loads. However, most of the power was supplied for the loads during the spring and winter seasons. Results will differ if money was spent for more solar panels or less power was used for the year.

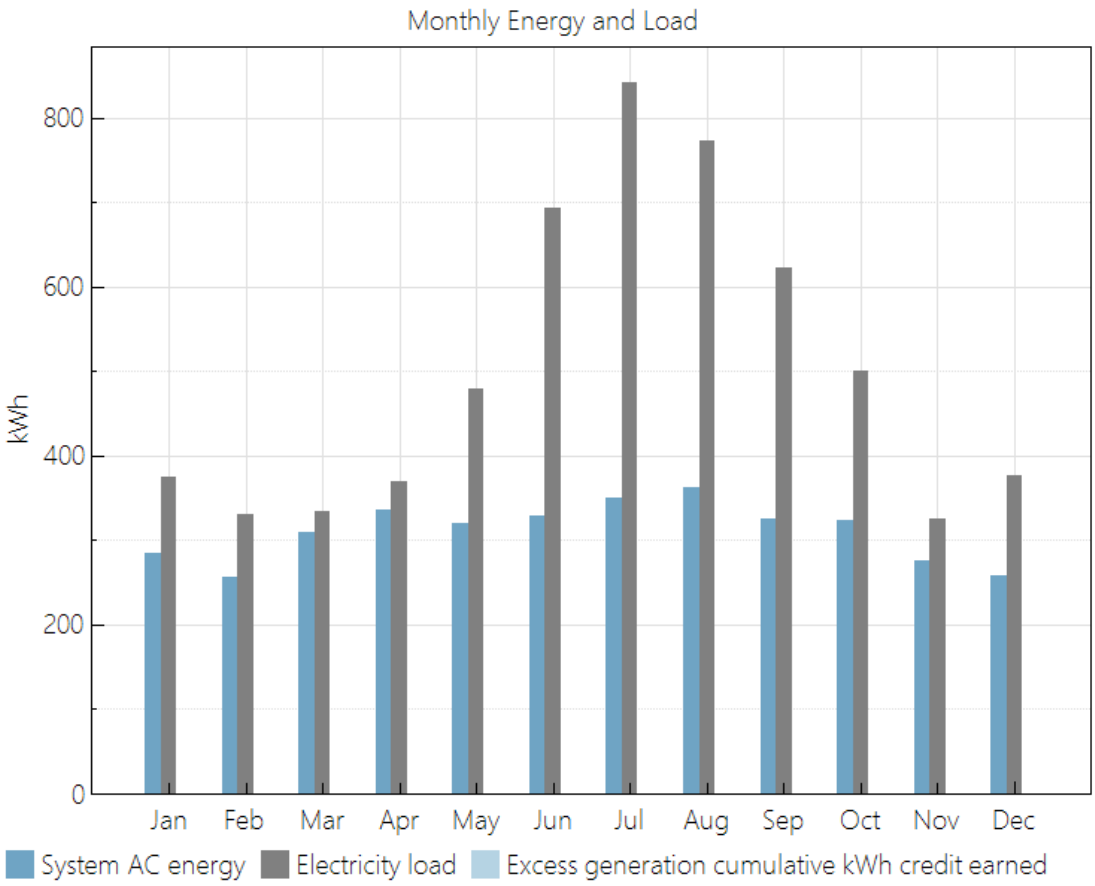

Figure 4.17 : SAM monthly energy and load graph

One of the last graphs that can be generated in SAM was the solar panel array power generated and load power for each month with respect to time. Figure 4.18, shows the breakdown of the power generated by the solar panel arrays and loads on average for 12 months. Within each month was the average of these two values represented in a 24-Hour manner. The data was useful to see what part of the day generated the most power and consumed most power for each of the 12 months. In the figure, the blue line was the load energy consumption and the orange line were the solar panel array power generation.

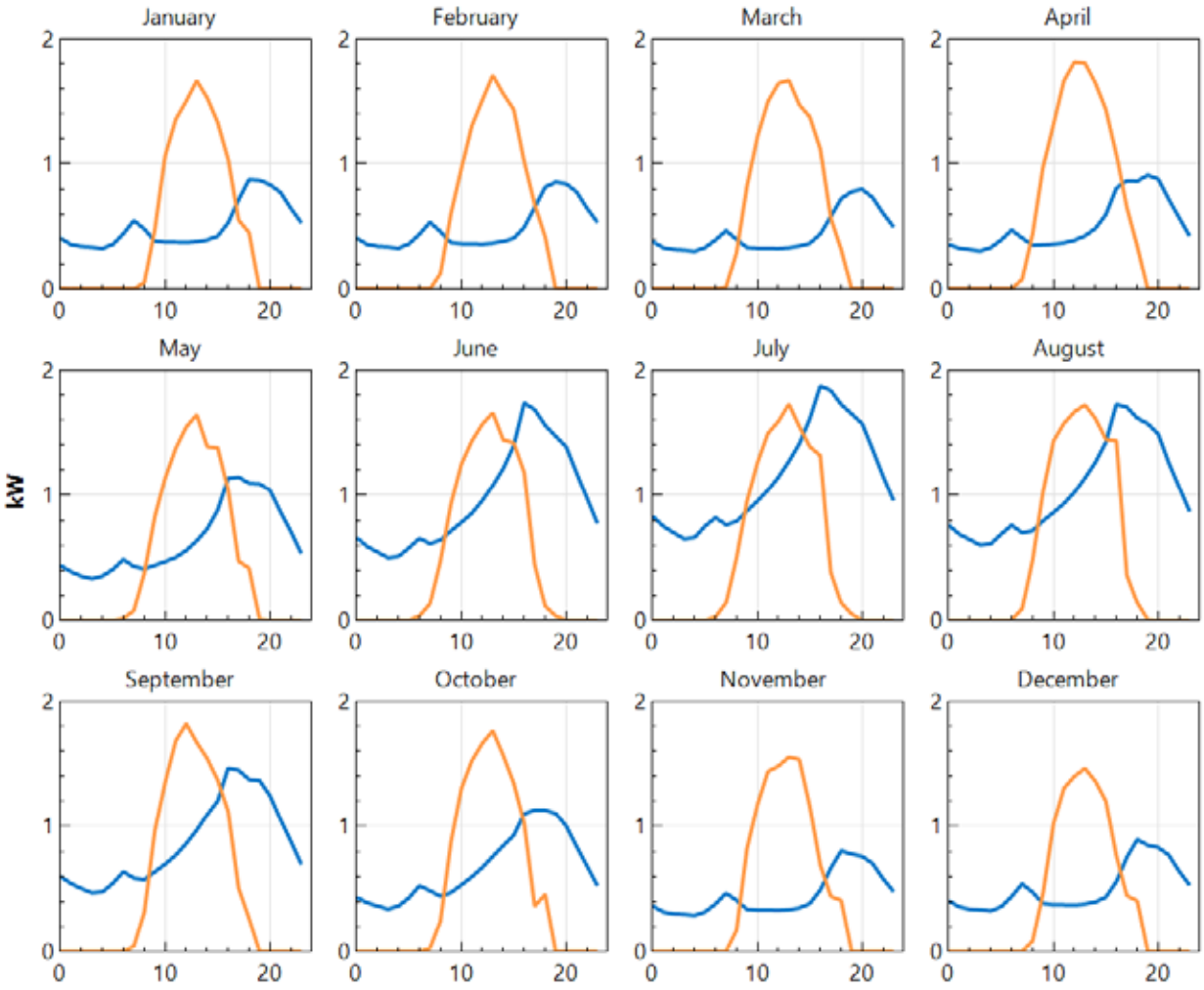

Figure 4.18 : SAM monthly solar array and load energy vs. time graphs

CHAPTER 5

PHYSICAL MICROGRID MODEL DATA

5.1 Isolated Nodes (No Microgrid)

To better understand the benefits of a microgrid, it was decided to gather data on how individual nodes work by themselves without sharing power. Individual nodes data would simulate a normal house currently found in the market, or a house that had a renewable generator, charge controller, batteries, inverter, and loads. This would be a house disconnected from the main grid and a house that cannot access power from other houses or any renewable generating systems. The data was logged using the TriStar's logger function as a computer runs the program MSView. The data was then stored in a CSV file and graphs where generated using Excel.

5.1.1 Rainy Day – No Loads – Large Node

Subsection 5.1.1 data collected from Node 3 (Large Node) of the microgrid that had generation capacity of 1.28 kilowatts and a battery bank of 450 Ah will be discussed. The first part of the data collected was with the batteries not connected to any loads, and the solar panels generating power on a cloudy and rainy day. It simulates the worst possible scenario of an isolated single generating system can experience because the solar panels cannot produce much power on a cloudy and rainy day and there was no place for the power to flow since there was no load. Figure 5.1, graph generated shows the input current, voltage, and power from the solar panels to the charge controller and the output current, voltage, and power from the controller to the battery bank. Data was taken from 10 AM to 5 PM.

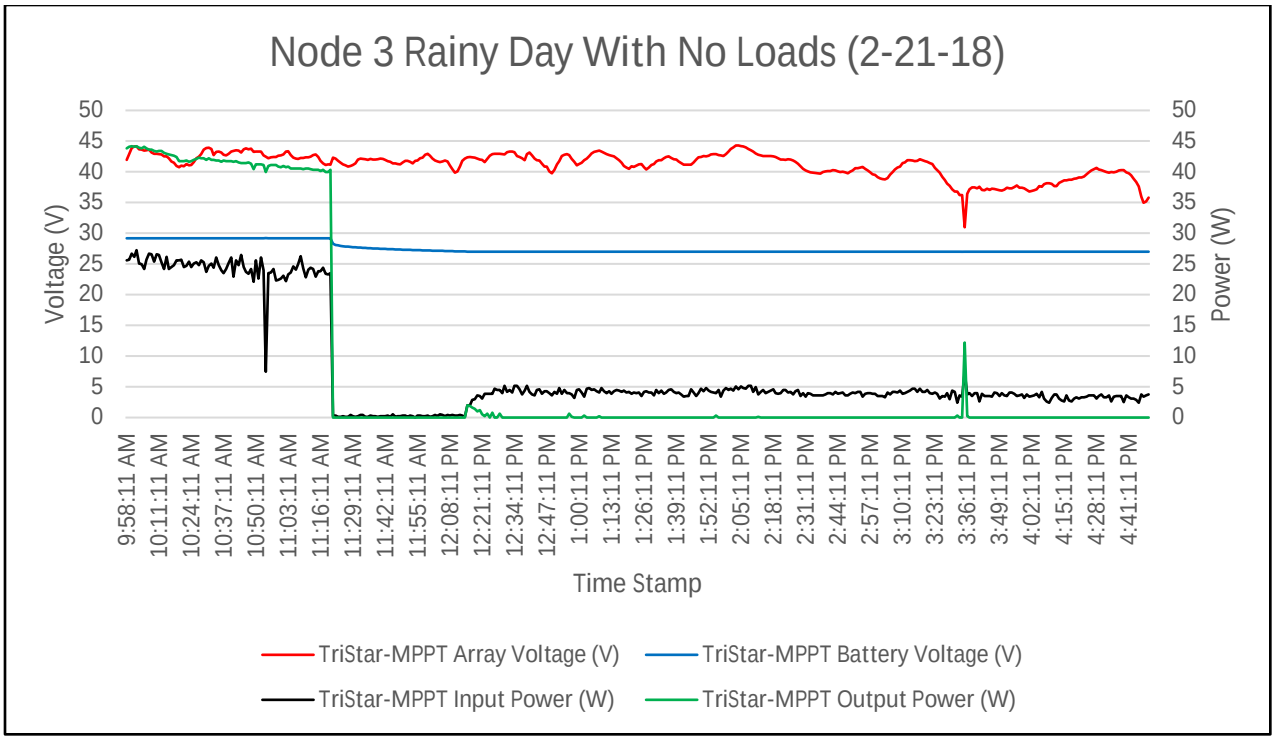

Figure 5.1 : Excel graph of node 3 (large node) rainy day with no loads

The data collected and displayed in Figure 5.1, it shows the voltage and current coming from the solar panels does not stay constant. It also shows the voltage going to the batteries from the charge controller was very consistent which means the voltage was changing constantly from the panels and the charge controller was trying to keep the voltage constant to the battery bank. MPPT charge controllers took the total power from the solar panels and changed the current to the battery banks while keeping voltage constant. Figure 5.1 shows the current and power changes with respect to the change in the input and output voltages. The last thing to note was the graph shows a sudden drop in current and voltage for the input and output of the system. It happened as the charge controller changed states when it saw the battery bank had reached peek voltage. Charge controllers do it to protect the battery banks from being overcharged and damaged.

5.1.2 Rainy Day – No Loads – Small Node

Subsection 5.1.2 discusses the data acquired when reading the smaller node during a rainy day with no inputs showing how the data of the smaller two nodes compares with the data from the one larger node. Data was collected from 10 AM to 5 PM, like the large node, but on a different day. The input and output current, voltage, and power of the node was seen in Figure 5.2.

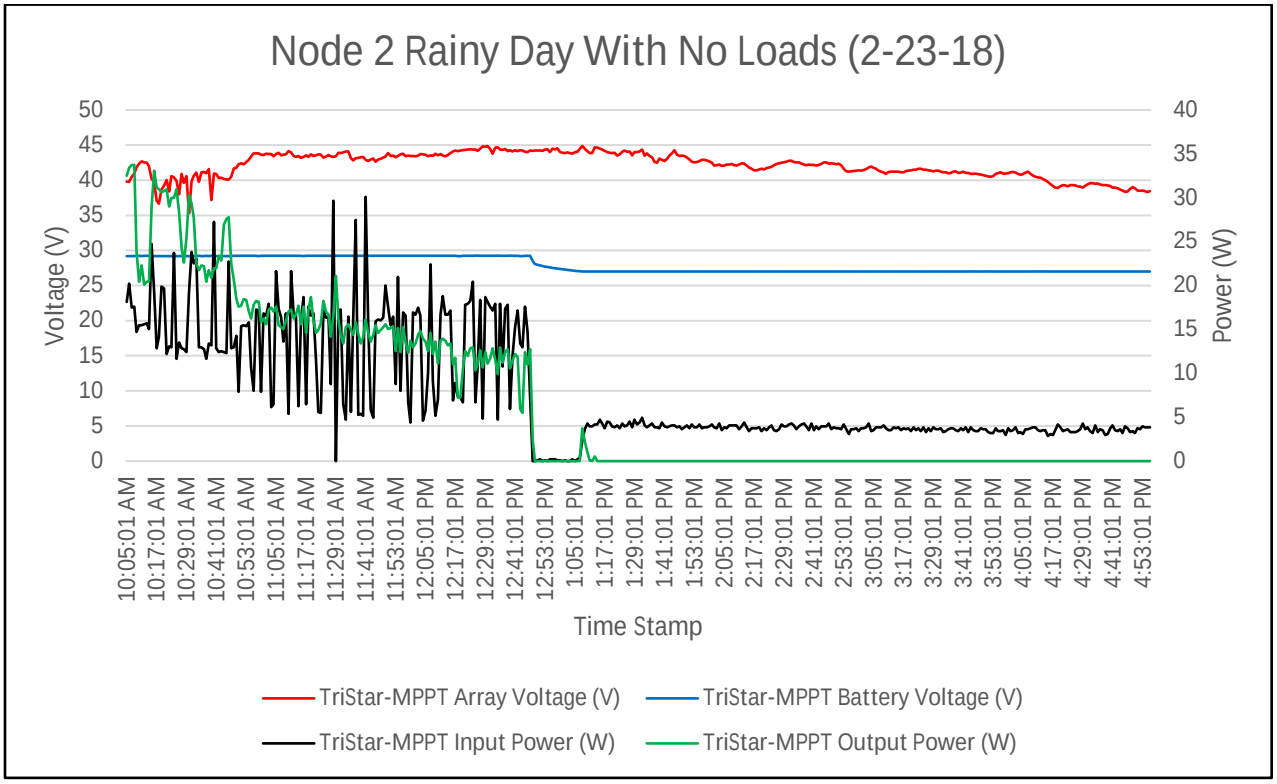

Figure 5.2 : Excel graph of node 2 (small node) rainy day with no loads

From the data, one can see a common relationship with the larger node with respect to the input and output voltage being close to the same. They do differ by the input and output current and power being closer together. Due probably because less power was being generated. Another thing that was different as the controller for the small nodes changes states later caused by many different factors, but, most likely, because the battery bank for the small node was one third the

size of the larger node using half of the number of solar panels. This would make the smaller nodes to need more time and power to charge.

5.1.3 Sunny Day – No Loads – Large Node

Subsection 5.1.3 showed the data collected from the large node on a sunny day when there are no loads, as seen in Figure 5.3. A sunny day made the large node generate more power than a cloudy/rainy day, as seen in Figure 5.1. The data in Figure 5.3 was taken on a different day then Figures 5.1 and 5.2, and the time was from 10 AM to 4 PM.

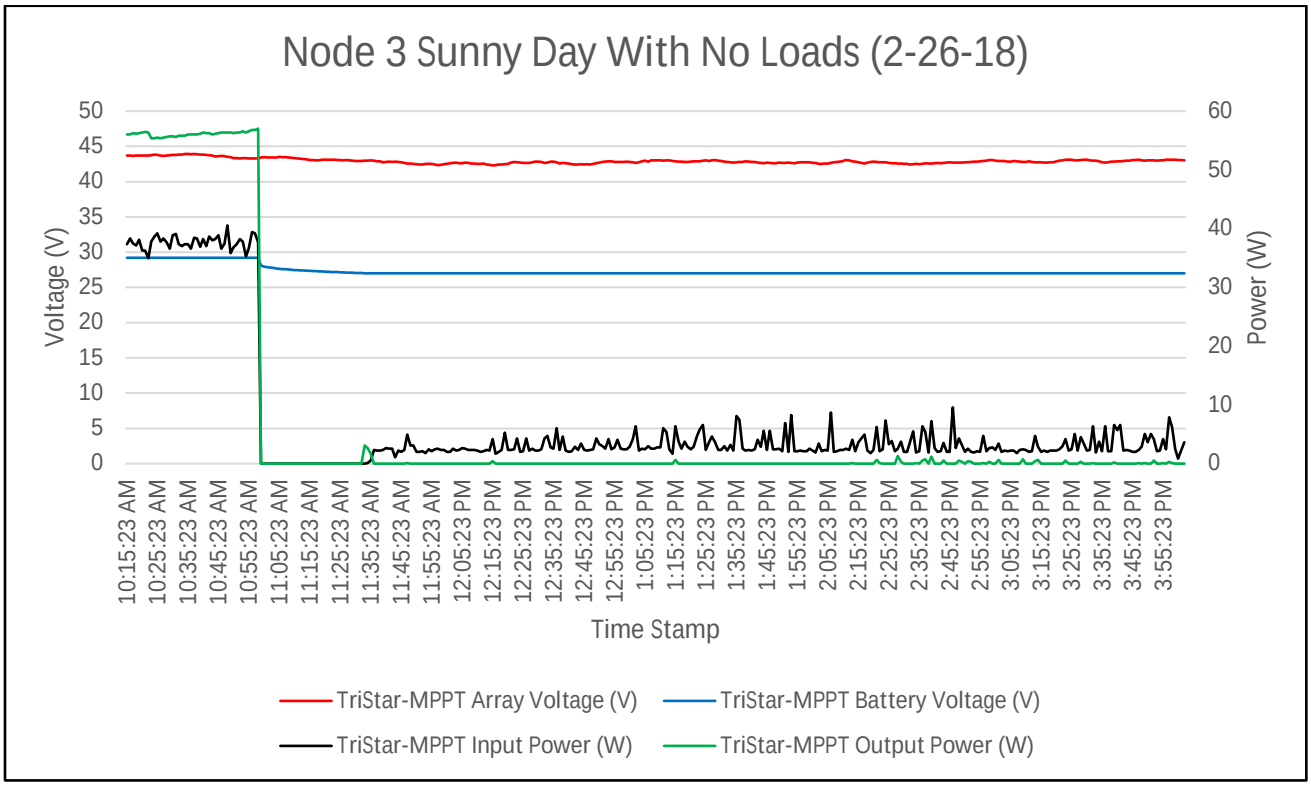

Figure 5.3 : Excel graph of node 3 (large node) sunny day with no loads

Looking at the data from Figure 5.3, one can see how the amount of sun during a day affects the large node. The voltage was especially interesting because the voltage coming from the solar panels was more consistent. This, in turn, made the current more consistent and stable

from the charge controller to the battery bank. Another thing to note was the controller changes states even sooner than in Figure 5.1 because, with more power being generated, the battery charges current to the battery bank reached its optimal charge voltage quicker.

5.1.4 Sunny Day – No Loads – Small Node

Subsection 5.1.4 references Figure 5.4, which was the graph of the small node during a sunny day without any loads. Data was taken on a different sunny day than Figure 4.3 but was taken during the same time of 10 AM to 4 PM. The data compared to Figure 4.3 showed its differences and similarities for the same timeframe.

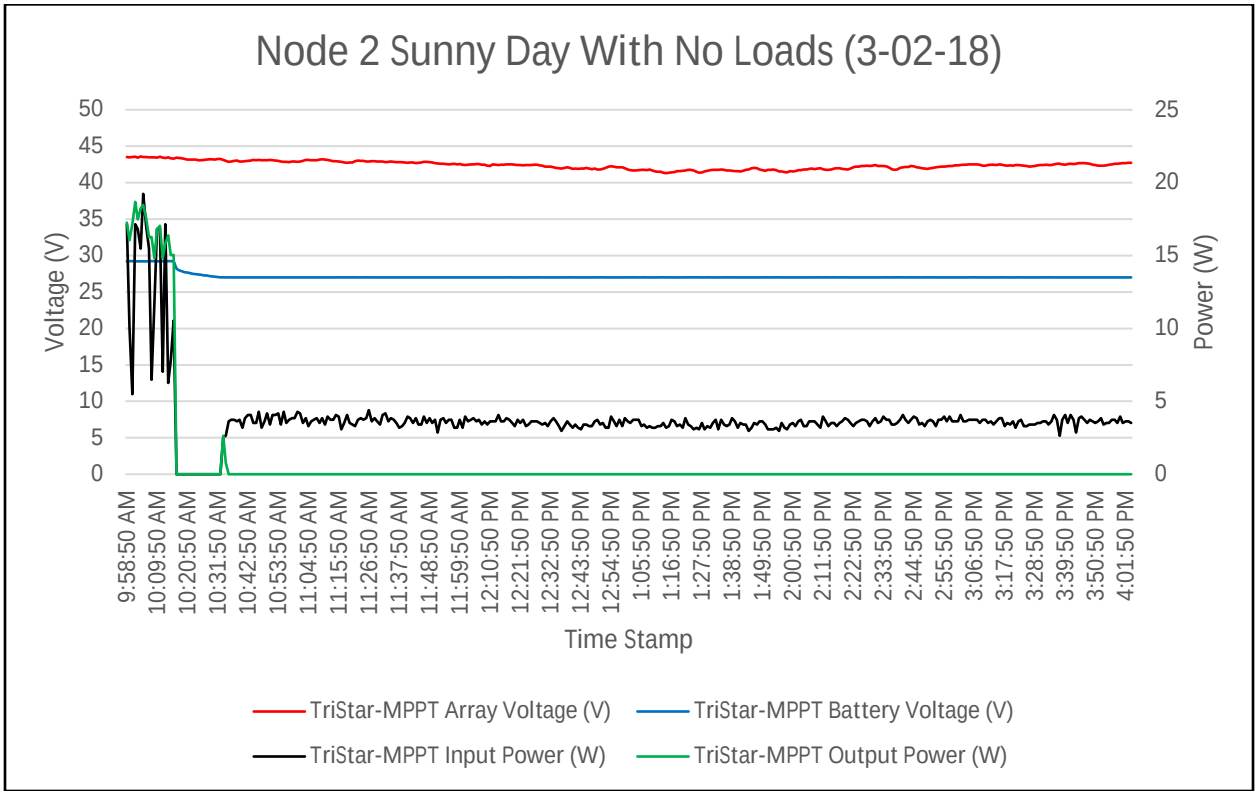

Figure 5.4 : Excel graph of node 2 (small node) sunny day with no loads

Looking at the data from Figure 5.4 like the large node, the small node has stable input and output voltage when there was a lot of sun and was unlike what happened in Figure 5.2

during a cloudy/rainy day; which in turn shows solar panels run more effectively on sunny days. The current and power drop off earlier than in Figure 5.2, as well, meaning the charge controller changed states earlier in the day. Which also happened to the large node when comparing Figures 5.1 and 5.3. As to be expected, the amount of power being generated from the arrays and the power being supplied to the batteries was smaller than the large node.

5.1.5 Sunny Day – With Loads – Large Node

When the large node was connected to a 1000W load there are a few things to note, as seen in Figure 5.5. The data shown in Figure 5.5 was collected from 10 AM to 4 PM during a sunny day.

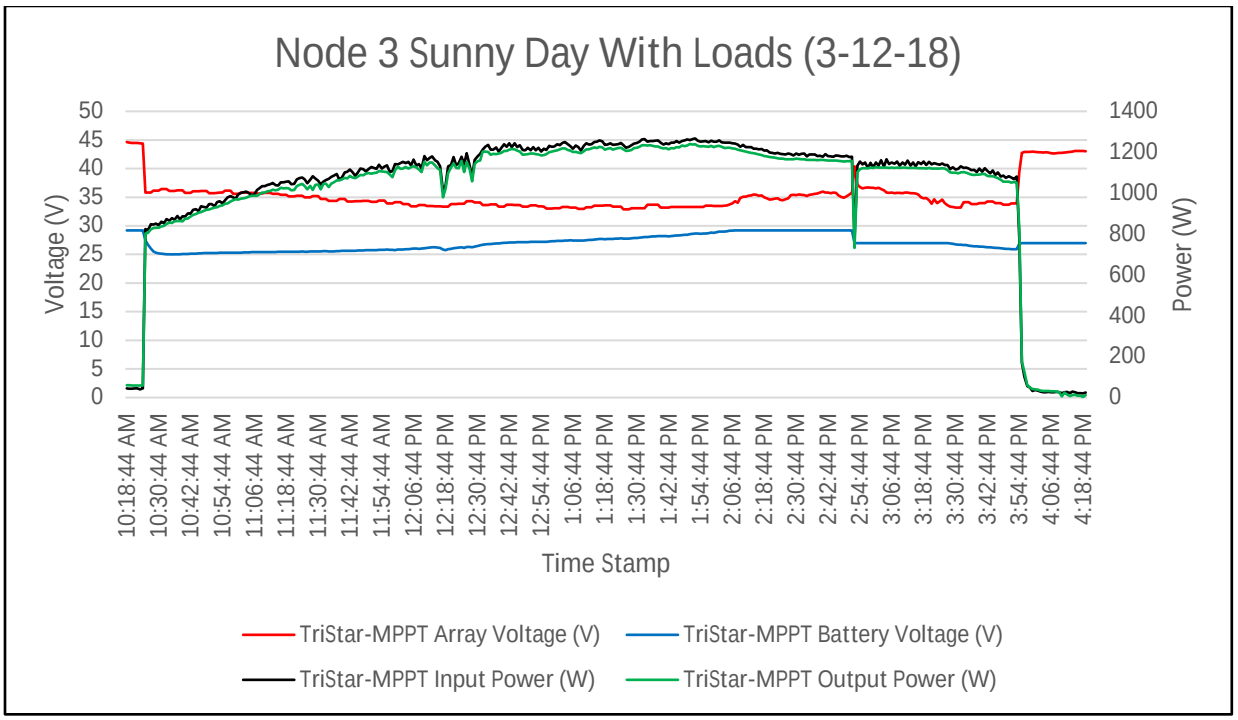

Figure 5.5 : Excel graph of node 3 (large node) sunny day with loads

Looking at the data in Figure 5.5, the amount of power being supplied by the solar panels and the power transferred to the battery banks was rather similar. Which means that the solar

panels have the capability to supply most of the power that was needed to power the loads and charge the batteries. The power slowly increases as the day continues because when the sun was at its peak the greatest amount of solar energy can be harnessed and supplied to charge the batteries, as well as, power the loads. The last thing to note was the sudden increase at the beginning of the graph and the sudden drop at the end of the graph. These shifts are caused by turning on and off the loads to the nodes. When the loads are not connected, the batteries are already at full charge and do not need more charge.

5.1.6 Sunny Day – With Loads – Small Node

The next data chart to look at is Figure 5.6, which shows the data for the small node when there was a sunny day and there are loads being powered. The data acquired was taken on a different day from Figure 5.5 but was also taken from 10 AM to 4 PM.

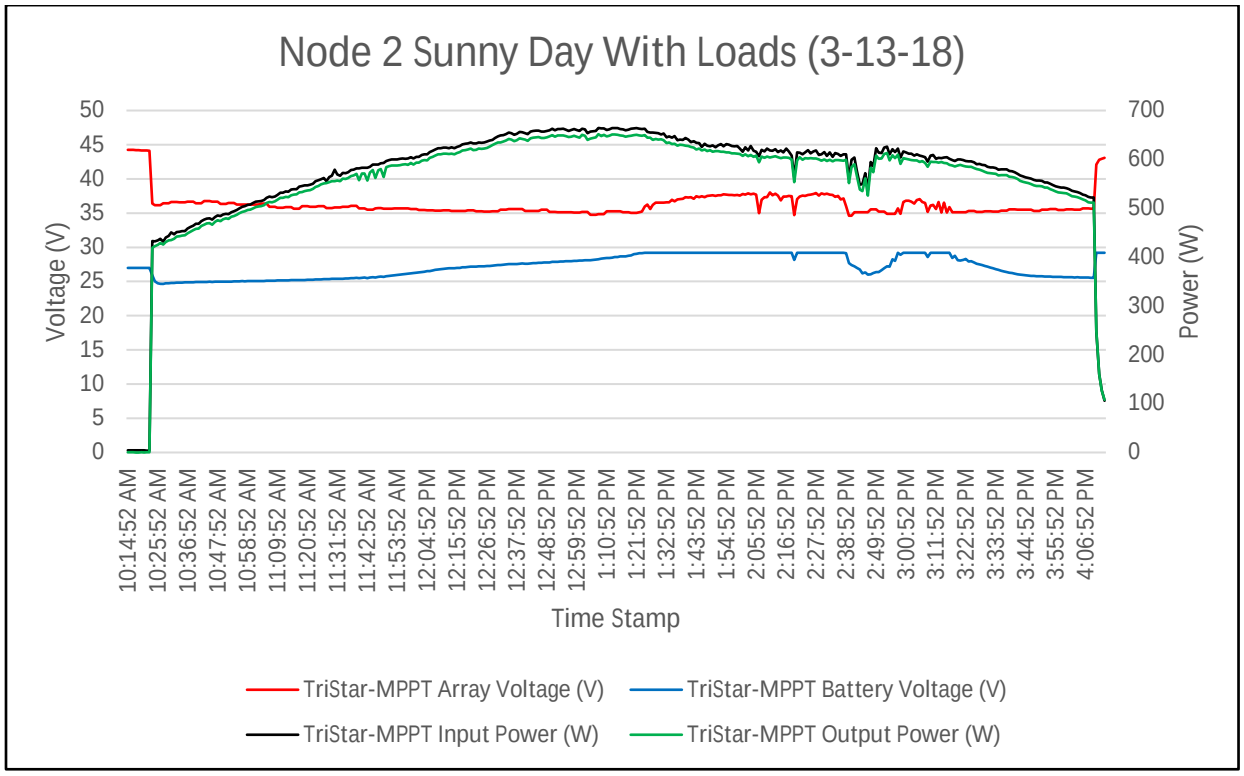

Figure 5.6 : Excel graph of node 2 (small node) sunny day with loads

From the data acquired, Figure 5.6, many things are like the data taken from Figure 5.5. It was shown that the small node also could supply most of the power to the 500W load, as well as, charge the battery banks during the peak solar production of the day. The main difference is not as much power is needed since the load was smaller. In addition, the graph shows the beginning and end that the power drops close to zero. Like in Figure 5.5, there are no loads connected and the battery banks are already fully charged. After comparing the data in Figure 5.6 and 5.5, it was proven that during a sunny day the individual nodes could operate independently.

5.2 Combined Nodes (Microgrid)

The data collected in Figures 5.1 to 5.6, shows that the small and large nodes can operate on their own. Which means that the nodes can function correctly when each one of them have no damage. In other words, none of the solar panels is disconnected and the system can work in an ideal situation. For this thesis, findings are discussed about how these nodes can operate when connected and when one of the smaller solar arrays was shut down. The shutdown of one of the node's solar panels would mean that node would eventually run out of stored power in the battery banks. However, if a microgrid system was implemented, power can be shared by solar arrays from other nodes and is what makes microgrids resilient during catastrophic events.

5.2.1 Sunny Day – With Loads – Large Node

When all nodes, small and large, were connected to the microgrid was when the data started to look interesting. Figure 5.7 showed the data collected from the large node from 9 AM to 4 PM during a sunny day.

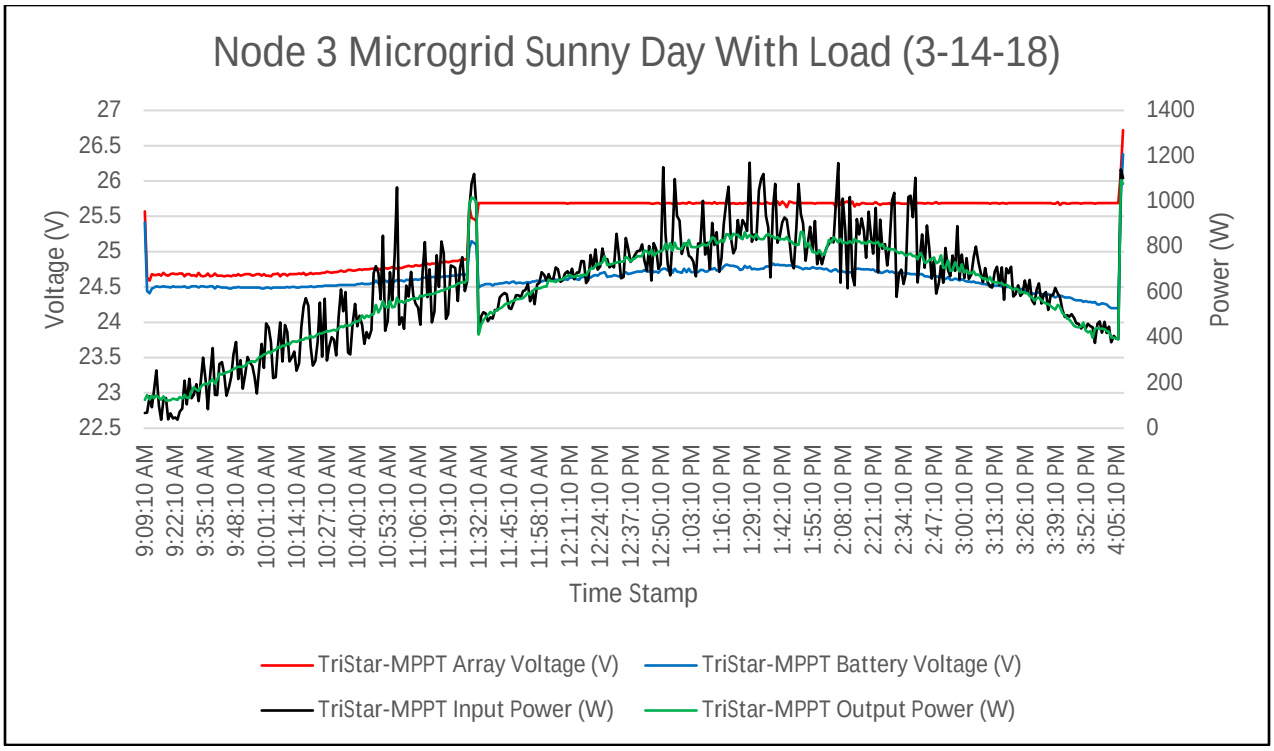

Figure 5.7 : Excel graph of node 3 (large node) sunny day with loads using microgrid

The data, in Figure 5.7, first shows a gradual increase in power because the loads were turned off and the charge controller was charging the battery banks. Then there was a sudden spike, which was caused by turning on all the loads for all the nodes in the microgrid. After that spike, the power being supplied to the charge controllers and battery banks had a curve. The power curve was like the curve found in Figure 5.5, but the power supplied was less because the power being supplied by the solar panel arrays were being shared with multiple nodes instead of just one. At the end of the graph, another spike was seen because the loads were turned off. During this period, the loads being off, the charge controllers were recharging the battery banks since the battery banks were supplying the necessary extra power the solar panels could not supply to the loads.

5.2.2 Partly Cloudy Day – With Loads – Small Node

In Figure 5.8, the graphed data for the small node is shown. Data was taken from 10 AM to 5 PM on a partly cloudy day and the loads where turned on in the microgrid.

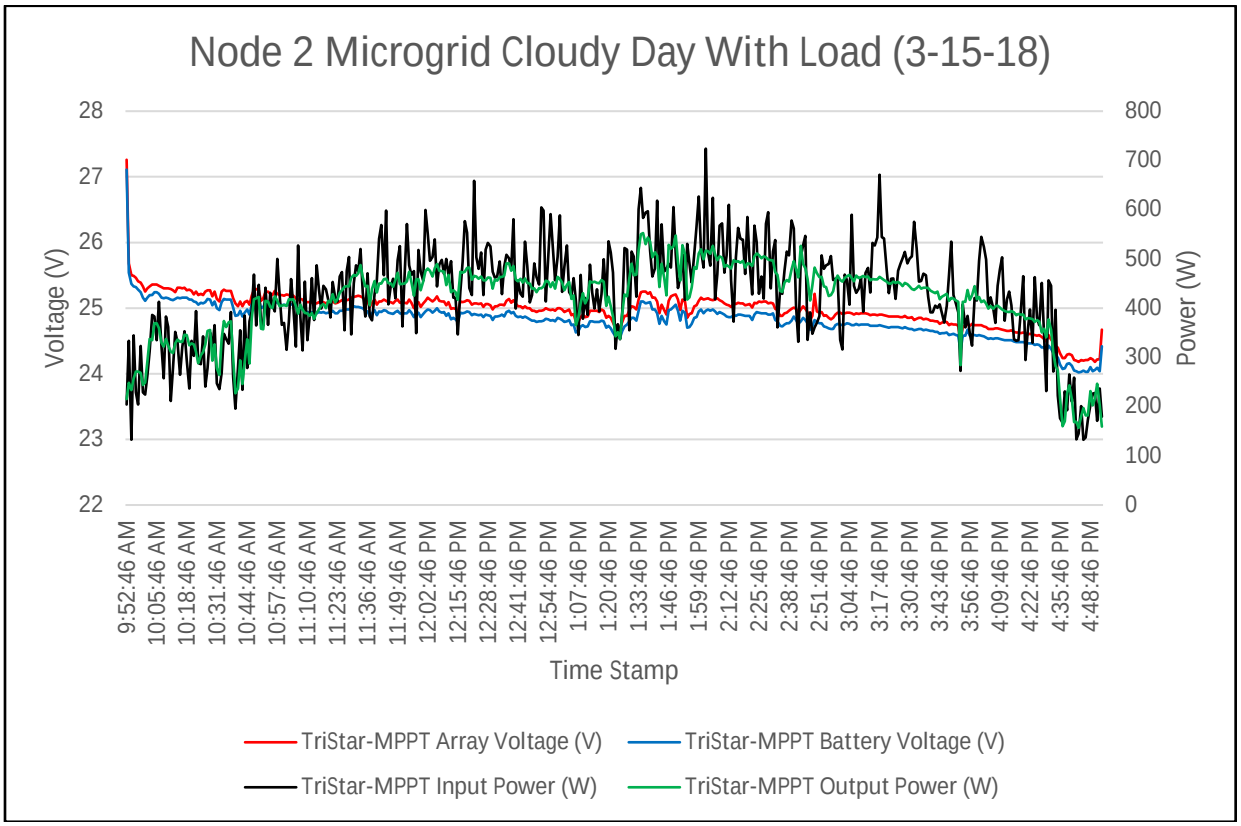

Figure 5.8 : Excel graph of node 2 (small node) partly cloudy day with loads using microgrid

Analyzing the data shown in Figure 5.8, the power being supplied by the solar panels and battery banks was curved. The power curve was like the curve in Figure 5.6 when the node was not in a microgrid configuration. The curve does have more interference in it shown by the oscillating line. However, the power curve does still show the same shape of increasing and decreasing power with respect to the amount of sun throughout the day. Figure 5.8 and Figure 5.7 are similar because the power curve of the small node when connected in a microgrid had less power than when it was connected on its own, likely caused by the cloudy weather, that

makes the power curve oscillate when the charge controller was changing states with respect to the cloud cover.

5.2.3 Sunny Day – With Loads – Small Node – Small Array Shutdown

Using the data shown in Figure 5.9, the main idea of a resilient microgrid was proven. The data collected in Figure 5.9 was during a sunny day, with all nodes having loads connected. Then one of the small solar arrays was shut down and the data was collected from the small node.

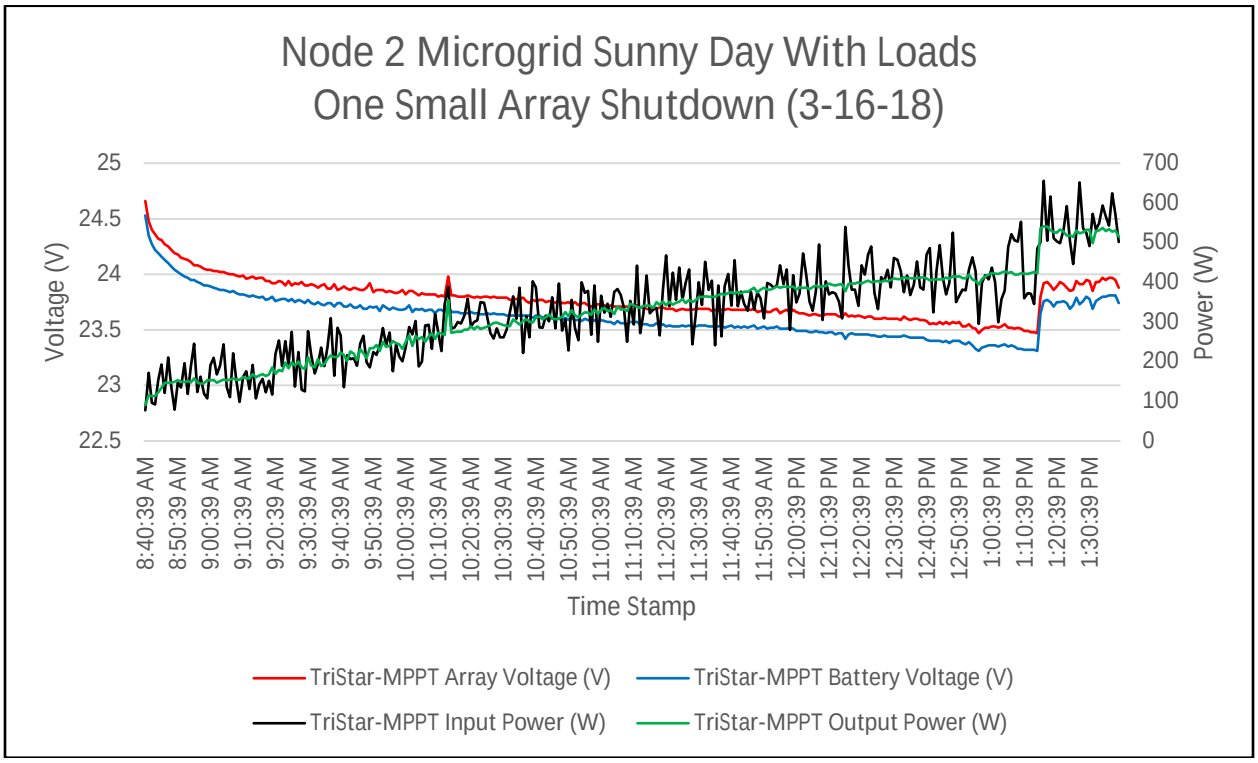

Figure 5.9 : Excel graph of node 2 (small node) sunny day with loads using microgrid and one small solar array shutdown

This thesis demonstrates that a microgrid was resilient against possible power shutdowns in Figure 5.9. For instance, when the small node's solar array had been damaged, and did not function, the node could only supply the amount of power that was stored in its battery banks.

However, as the data shows, in Figure 5.9, when the node was connected to a microgrid the node can still have access to power. The data in Figure 5.9 were acquired from 8:30 AM to 1:30 PM and shows a steady increase in power to the small node. Which supports the idea that power was being shared by the other solar panel arrays that were still connected to the microgrid.

CHAPTER 6

CONCLUSION AND FUTURE IMPLEMENTATION

6.1 Conclusion

Looking at the simulation made in Simulink for a microgrid to be resilient, there needs to be a way to share power to multiple loads in the microgrid. This is different from an isolated power system because if a solar panel array was shutdown at one of the modules, the module has no other way to supply power to the loads except through the stored power in its battery banks. However, the stored power can only last for a given time unless another power generator is available.

The creation of a physical model of a microgrid and testing proves that sharing power to multiple nodes was more resilient than an isolated system. Looking at the data in Figure 5.9, we conclude that even when one of the solar panel arrays was shut down there was still power being supplied to the node. This means that the microgrid has the infrastructure to supply power to multiple nodes even when different power generators were disabled and makes the microgrid more resilient against natural disasters which can disable renewable generators or the main grid at any time. Both the simulations and physical model of the microgrid support the same conclusion, a microgrid was resilient against all power loss to a single node when that node's main power supply was disabled.

During catastrophic events, neighborhoods and local businesses utilizing a microgrid would continue to have access to power when the main grid or individual renewable generators are shut down. For example, if Houston had the microgrid infrastructure in place when Hurricane Harvey hit in August 2017, homes and businesses would not have been completely without power. This would be a result of neighborhoods and multiple buildings continuing to

generate and supply power within the microgrid if the main grid was damaged. In addition, the microgrid would continue to provide power to homes and buildings with damaged generators within the microgrid. The vision for this thesis was to prove the resilience of a microgrid and show the benefits of restructuring the current power system to a microgrid to prevent power loss in the event of a natural disaster.

6.2 Future Implementations

This thesis focused on resiliency of the microgrid, there are many more aspects that merit further studies. One aspect is reliability, [2]; does the microgrid supply a consistent reliable power to the loads? The main grid is always being monitored because of the demands of consumers of electricity wanting power for their devices. The loads can increase or decrease depending on the needs from the consumer. To study this, a researcher would need more measuring equipment to measure the voltage and current the loads are using in the microgrid. With this data, researchers can compare with how much voltage and current is being supplied by the renewable generators and battery banks.

Another point of interest of a microgrid is to make it a smart grid (virtual grid) [21]. Smart grids are an extension of microgrids adding sensors and controllers to control the flow of power in the microgrid. For instance, if your microgrid has some sensitive equipment running, they should have priority of the power in the microgrid. Therefore, a controller would act like a switch to supply most of the power to the most important node with the sensitive equipment. Accomplished by using controllers and sensors because the current microgrid, as discussed in this thesis, supplies an equal amount of power to all nodes. This allows the system to be resilient

against unforeseen shut downs from the grid or nodes in the microgrid. However, you cannot control where the power is going.

One other point worth some research is the power quality of the microgrid [2]. Which is important if you are making an AC microgrid. In this thesis, it mainly focused on making the microgrid DC with inverters at the load. Yet, if you wanted to implement a microgrid in an area that was already reliant on AC power, there are many factors to keep in mind. For instance, when generating power and combining power to an AC microgrid, you need to keep the frequencies of the AC power consistent. If there was no consistency, most modern electronics which use AC power from the main grid will not function. In worst cases, it could permanently damage the electronics. Another point of AC microgrids, as well as DC microgrids, is you need to keep the voltage consistent throughout all the nodes and devices. In this thesis model, 24 V was used, but other voltages such as 12 and 36 are common.

Microgrids are shown to be very resilient from this study; however, there are a few points in the microgrid, which could be further improved upon. One of the most common areas would be the efficiency of the components in the microgrid. It can range from the batteries, solar panels, windmills, and wire. For instance, improving the efficiency of the solar panels included in the physical model. Solar panels run the most efficient when their temperatures do not exceed 65 °C and there was no shading. However, during the TX summer time, when there was the most sun, there was also the hottest temperatures. For solar panels to be more efficient during these times, it was best to cool them down by water cooling stems mounted on the top of the panels. A further study on how much more efficient the panels would operate during these times, and, if that increased efficiency, justified using more equipment and power to cool the panels.

REFERENCES

[1] U.S. Department of Energy by the National Renewable Energy Laboratory, "Connecting Your Solar Electric System to the Utility Grid," July 2002. [Online]. Available: https://www.nrel.gov/docs/fy02osti/31687.pdf. [Accessed 20 January 2018].

[2] S. Parhizi, H. Lotfi, A. Khodaei and S. Bahramirad, "State of the Art in Research on Microgrids: A Review," *IEEE Access,* vol. 3, pp. 890-925, 2015.

[3] Y. Jiang-feng, W. Wei and P. Yong-gang, "A real-time optimal energy dispatch for microgrid including battery energy storage," *2016 10th International Conference on Software, Knowledge, Information Management & Applications (SKIMA),* pp. 314-318, 2016.

[4] A. Ellis, "Microgrids and Resilience Framework," in *IRED Symposium on Microgrids,* Niagara Falls, 2016.

[5] M. N. Faqiry and S. Das, "A Budget Balanced Energy Distribution Mechanism among Consumers and Prosumers in Microgrid," *2016 IEEE International Conference on Internet of Things (iThings) and IEEE Green Computing and Communications (GreenCom) and IEEE Cyber, Physical and Social Computing (CPSCom) and IEEE Smart Data (SmartData),* pp. 516-520, 2016.

[6] CU-ECEN4517, *3.1 PV panel Spice model and simulation,* YouTube, 2014.

[7] M. Assaad, "Arduino Based Hybrid MPPT Controller for Wind and Solar," University of North Texas, Denton, 2017.

[8] D. Andrea, "White Paper - Estimating the State Of Charge of Li-Ion batteries," Li-ion BMS , 10 January 2009. [Online]. Available: http://liionbms.com/php/wp_soc_estimate.php. [Accessed 11 March 2018].

[9] SamlexSolar, "Lead-Acid Batteries," SamlexSolar, [Online]. Available: http://www.samlexsolar.com/learning-center/lead-acid-batteries.aspx. [Accessed 04 Feb 2018].

[10] IBT Power, "Typical Lithium Ion Technical Data," IBT Power, [Online]. Available: http://www.ibt-power.com/Battery_packs/Li_Ion/Lithium_ion_tech.html. [Accessed 04 Feb. 2018].

[11] SunWize, "Solar Charge Controller Types," SunWize, [Online]. Available: https://www.sunwize.com/tech-notes/solar-charge-controller-types/. [Accessed 15 December 2017].

[12] ExplainThatStuff!, "Inverters," ExplainThatStuff, [Online]. Available: http://www.explainthatstuff.com/how-inverters-work.html. [Accessed 20 Feb 2018].

[13] R. Singh and M. Kirar, "Transient stability analysis and improvement in microgrid," *2016 International Conference on Electrical Power and Energy Systems (ICEPES)*, pp. 239-245, 2016.

[14] S. Heo, W. K. Park and I. Lee, "Microgrid design with renewable energy sources and storage based on power conditioning system for autonomous island operation," *2017 IEEE International Conference on Industrial Technology (ICIT)*, pp. 147-152, 2017.

[15] V. Krishnamurthy and A. Kwasinski, "Effects of Power Electronics, Energy Storage, Power Distribution Architecture, and Lifeline Dependecies on Microgrid Resiliency During Extreme Events," *IEEE Journal of Emerging and Selected Topics in Power Electronics*, vol. 4, no. 4, pp. 1310-1323, Dec 2016.

[16] CerroWire, "Ampacity Chart," CerroWire, 2014. [Online]. Available: http://www.cerrowire.com/ampacity-charts. [Accessed 11 March 2018].

[17] MathWorks, "Simscape Power Sytems," MathWorks, [Online]. Available: https://www.mathworks.com/products/simpower.html. [Accessed 01 September 2017].

[18] NREL, "System Advisor Model," National Renewable Energy Laboratory, [Online]. Available: https://sam.nrel.gov/. [Accessed 15 01 2018].

[19] F. Mohamed, "Microgrid Modelling and Simulation," pp. 1-81, 2006.

[20] H. Mita, "Simplified Model of a Small Scale Micro-Grid - MATLAB & Simulink," MathWorks, [Online]. Available: https://www.mathworks.com/help/physmod/sps/examples/simplified-model-of-a-small-scale-micro-grid.html. [Accessed 05 September 2017].

[21] M. S. Wang and B. Dong, "The Existed Problems and Possible Solutions of Distributed Generation Microgrid Operation," *2011 Asia-Pacific Power and Energy Engineering Conference*, pp. 1-4, 2011.